# Journal of Ethiopian Society of Chemical Engineers

## Main Featuers:

- Experimental Study on Portland Pozzolana Cement and Citric Acid Influence on Compressive Strength of Reinforced Concrete
- Investigating the possibility of producing Polyhydroxyalkanoates (PHAs) Using Hydrolysates of Napier grass by Burkholderia Sacchari strain
- Bio-butanol Production from Hydrolysates of Napier Grass Using Clostridium acetobutylicum: A Comparison of Separate and Semi-Simultaneous Fermentation Processes
- Enhancing Energy Security in Ethiopia through Natural Gas and Geothermal Development

**Journal of Ethioipan Society of Chemical Engineers(ESChE)**

**Volume I**

**Founded in November 1995**

**Website: www.eschenew.com**

**Tel: +251907929202**

**E-Mail: info@eschenew.com**

**P.O.BOX: 81264**

**Addis Abeba, Ethiopia**

## Contents

1. Experimental Study on Portland Pozzolana Cement and Citric Acid Influence on Compressive Strength of Reinforced Concrete, by: **Abebech Haileselassie and Sintayehu Nibret** 1

2. Investigating the possibility of producing Polyhydroxyalkanoates (PHAs) Using Hydrolysates of Napier grass by Burkholderia Sacchari strain, by: **Adane Bazezew and Sintayehu Nibret** 13

3. Bio-butanol Production from Hydrolysates of Napier Grass Using Clostridium acetobutylicum: A Comparison of Separate and Semi-Simultaneous Fermentation Processes, by: **Biruk Yohannes and Dr. Solomon Kiros** 25

4. Enhancing Energy Security in Ethiopia through Natural Gas and Geothermal Development, by: **Ramadan Ahmed** 39

**Editor's Note**

We do believe that as any other journal publisher, our society should have its own manuscript preparation guidelines for quality journal publication and for avoiding irregularities on submitted papers. The advantage of clear guidelines on manuscripts preparation is that they can be edited and prepared for publication without having too much retyping. This ESChE Manuscript Preparation Guidelines has been prepared for future journal volume preparations.

**Disclaimer:** ESChE isn't responsible for misrepresentations of the contents of papers presented in this journal volume.

**Manuscript Preparation Guidelines**

**Title:**

The title should be concise, clear, and informative, reflecting the main research question and key contribution of the study. Avoid jargon, unnecessary acronyms, and overly long wording. It should accurately represent the scope and focus of the research.

**Authors and Affiliations:**

Provide the full names of all authors in the correct order and ensure accurate spelling. Include institutional affiliations below the author names using superscripts where necessary. Provide the full address of each institution and, if possible, email addresses.

**Corresponding Author:**

Clearly indicate the corresponding author responsible for communication during submission, review, publication, and post-publication. Ensure that the contact details remain updated.

**Abstract and Keywords:**

The abstract (150–300 words) should briefly summarize the objective, methodology, main findings, and significance of the research. Immediately after the abstract, include up to six keywords representing the main themes of the study.

**Manuscript Structure:**

Organize the paper into clearly numbered sections such as Introduction, Materials and Methods, Results, Discussion, and Conclusions. The introduction should identify the research problem and gap in existing studies, methods should allow reproducibility, results should present findings clearly, and conclusions should summarize the main outcomes.

**Tables, Figures, and References:**

Tables and figures should be clearly labeled, numbered, and accompanied by captions. Equations should be written using an equation editor. All references cited in the text must appear in the reference list and follow a consistent citation style. Reference management tools such as **Mendeley** or **EndNote** are recommended.

For detailed instructions to authors, please visit our website at
https://www.eschenew.com/publications-resources/

# Experimental Study on Portland Pozzolana Cement and Citric Acid Influence on Compressive Strength of Reinforced Concrete

**Abebech Haileselassie[1] and Sintayehu Nibret Tiruneh[1,2*]**

[1]Center for Materials Science and Engineering, Addis Ababa University, P.O. Box 385, Ethiopia
[2]School of Chemical and Bio engineering, College of Technology and Built Environment, Addis Ababa University, P.O. Box 385, Ethiopia

*Corresponding Author: Sintayehu Nibret Tiruneh
(Email: sintayehu.nibret@aait.edu.com)

**Abstract**

In Ethiopia, the construction industry relies heavily on Ordinary Portland Cement (OPC) for structural applications due to its rapid early strength development. However, the widespread use of OPC contributes to high production costs and increased carbon emissions associated with cement manufacturing. Therefore, there is a growing need to evaluate more sustainable alternatives, such as Portland Pozzolana Cement (PPC), potentially enhanced with organic admixtures, to meet structural performance requirements while reducing environmental impact.
This study investigates the combined effect of partially replacing [1]Ordinary Portland Cement (OPC) with [2]Portland Pozzolana Cement (PPC) and adding citric acid as a chemical admixture on the compressive strength, setting time, and workability of reinforced concrete. Concrete samples of C-30 grade were prepared using OPC, PPC, and PPC modified with varying dosages of citric acid (0.1–0.4% by weight of Portland Pozzolana Cement). Experimental results indicated that citric acid acts as a retarder and water-reducing agent, improving the workability and extending the setting time without significantly compromising strength. The optimal dosage was determined to be 0.3% citric acid, which resulted in a 55% increase in slump, a delay in setting time of 1 hr 50 min (initial) and 3 hr 10 min (final), a comparable 28-day compressive strength to OPC mixes and a cost reduction of 258.86 Ethiopian birr per cubic meter of concrete. The combined use of PPC and citric acid demonstrated improved performance and cost effectiveness compared to OPC-based mixes, promoting sustainable concrete production suitable for the Ethiopian construction industry.

**Keywords:** Portland Pozzolana Cement (PPC); Citric Acid; Reinforced Concrete; Compressive Strength; Mix Design

## 1. NTRODUCTION

Concrete is the most extensively used construction material worldwide, primarily valued for its compressive strength, durability, and adaptability. In Ethiopia, Ordinary Portland Cement (OPC) dominates structural applications because of its rapid early-age strength development, whereas Portland Pozzolana Cement (PPC) is mainly employed in non-structural works due to its slower strength gain (Addisu, 2014; Rajendra, 2013).

However, the energy-intensive manufacture of OPC contributes substantially to $CO_2$ emissions, prompting global interest in more sustainable alternatives that balance environmental and performance demands.
PPC, composed typically of 70 % clinker, 25 % pozzolana (often pumice or volcanic ash in Ethiopia), and 5 % gypsum, offers lower heat of hydration and improved durability through secondary C-S-H formation from pozzolanic reactions. Despite these advantages, the slower

hydration of PPC limits its use in reinforced concrete, where early strength is critical. To overcome this limitation, attention has turned to chemical admixtures capable of modifying cement hydration and workability. Among them, citric acid—an organic compound classified under ASTM C494 as a Type D water-reducing and retarding admixture—has shown potential to delay hydration while enhancing dispersion and flow ability (Tinnea & Young, 1977a; Purnomo et al., 2019a). At optimized dosages, citric acid can improve the microstructural compactness of cement paste and reduce water demand, but excessive quantities may cause undue retardation or strength loss.

In Ethiopia's hot climate, ready-mixed concrete often faces challenges of premature setting during transportation and placement. Controlled retardation through admixtures such as citric acid can provide additional handling time without compromising final strength. While PPC contributes to long-term durability and reduced $CO_2$ emissions, its interaction with citric acid in reinforced concrete remains largely unexplored. Previous research on Ethiopian cements (Addisu, 2014; Nigus, 2005) focused mainly on comparing OPC and PPC without chemical enhancement, revealing that PPC achieves lower 28-day strength but superior impermeability and sulfate resistance. Other studies (Dhanya Sathyan, 2018; Purnomo et al., 2019b) confirmed that appropriate admixture selection and dosage optimization can substantially improve the performance of PPC-based concrete.
Recent research has explored advanced uses of Portland Pozzolana Cement (PPC) and chemical admixtures to enhance concrete performance. Albadrani (2025) demonstrated that PPC blends with rice husk ash (RHA) achieved improved long-term compressive and flexural strength, highlighting the role of supplementary cementitious materials in sustainable concrete design.

In related work on admixture effects, Qin et al. (2024) investigated citric acid-modified chitosan and found that it extended setting times and influenced strength and shrinkage behavior, suggesting that citric acid derivatives can modulate hydration kinetics and durability performance. Ciacchella et al. (2025) further expanded the application of citric acid in concrete by demonstrating its effectiveness as a salt crystallization inhibitor under wet–dry cycles, linking citric acid chemistry to enhanced durability against environmental stress.

This work builds upon the findings of Meseret Simachew (2021), whose study "Study on Application of Portland Pozzolana Cement for Structural concrete" established the local context and technical limitations for using PPC in Ethiopian reinforced concrete. Furthermore, the study by Zhu, Yu, and Li (2021) serves as a critical recent contribution, demonstrating that citric acid serves as an effective admixture to significantly improve the injectability, workability, and flowability of cementitious systems.

Recent studies have increasingly focused on sustainable and high-performance concrete through the use of supplementary cementitious materials and chemical admixtures. Albadrani (2025) demonstrated that incorporating rice husk ash into PPC concrete improves long-term compressive strength due to enhanced pozzolanic reactions. Qin et al. (2024) investigated citric acid-modified chitosan and reported delayed setting times and enhanced later-age strength, showing the impact of citric acid-based admixtures on hydration kinetics. Ciacchella et al. (2025) highlighted citric acid's role in reducing durability-related cracking under salt crystallization conditions. Collectively, these findings provide updated insights into the interactions of PPC and chemical admixtures. Theoretical frameworks based on cement hydration kinetics, pozzolanic reactions, and admixture effects on microstructure formation inform our experimental approach and highlight the practical relevance of optimizing mix designs for reinforced concrete performance.

While previous studies have separately investigated Portland Pozzolana Cement (PPC) and citric acid as a chemical admixture, there is no experimental evidence on their combined influence on the compressive strength of reinforced concrete under varying mix proportions. Therefore, the key research question of this study is: How does the combined use of PPC and citric acid affect the compressive strength development of reinforced concrete, and what are the optimal mix conditions for maximizing performance? Addressing this question provides practical guidance for mix design and contributes to the understanding of PPC–citric acid interactions in reinforced concrete.

The study seeks to provide a scientific basis for understanding the synergistic interaction between PPC and citric acid and how this combination influences the ydration process, strength development, and fresh-concrete behavior. In doing so, it addresses one of the most pressing challenges in Ethiopian h construction—achieving both economic efficiency and environmental sustainability without compromising structural quality.

In Ethiopia's construction industry, it's becoming increasingly common for PPC (Portland Pozzolana Cement) not to be the preferred choice for making reinforced concrete. Many consider PPC to be a less effective type of cement because it takes longer to reach the same strength as OPC (Ordinary Portland Cement). Therefore, this study focuses on examining how mixing PPC as a partial replacement for OPC and citric acid affects reinforced concrete, particularly in achieving the desired compressive strength after 28 days, and in reducing concrete cost. This research addresses the lack of experimental data regarding the combined use of PPC and citric acid to evaluate their suitability and effectiveness in reinforced concrete construction.

The specific objectives of the study are threefold: (i) to determine the optimum citric acid dosage that maximizes the performance of PPC-based concrete by improving its fresh and hardened properties; (ii) to evaluate the combined influence of PPC and citric acid on setting time, workability, and compressive strength, thereby quantifying their synergistic impact; and (iii) to develop a practical and locally adaptable concrete mixture that can be implemented within Ethiopia's construction sector to reduce cement consumption, production costs, and carbon emissions. Furthermore, the study seeks to contribute to the broader body of sustainable construction knowledge by providing a data-backed methodology for integrating organic admixtures into blended cement systems. Ultimately, this research not only offers an alternative approach to improving PPC performance but also supports the transition toward greener and more durable concrete technologies suited to Ethiopia's environmental and industrial context.

Although the use of citric acid as a retarding admixture in cementitious systems has been reported in previous studies, and Portland Pozzolana Cement (PPC) has also been extensively investigated independently, prior research has generally examined these materials separately. In addition, some studies have explored the combination of PPC with various chemical admixtures other than citric acid. However, the specific combined effect of citric acid with locally produced Ethiopian PPC has not been systematically investigated for normal-grade structural applications. To the best of the author's knowledge, no prior research has comprehensively evaluated the synergistic interaction between PPC and optimized citric acid dosages in reinforced concrete. Therefore, this study presents original experimental work aimed at examining how controlled citric acid incorporation influences early-age and later-age compressive strength development of PPC-based concrete, with the objective of enhancing its structural applicability and cost-effectiveness as a sustainable alternative to OPC.

## 2. MATERIALS AND METHODS

### 2.1. Experimental Overview

All laboratory work was conducted at the Addis Ababa University, College of Technology and Built Environment (Materials Testing Laboratory) and Yencomad Construction PLC Laboratory. The investigation involved raw-material characterization, concrete mix design, specimen preparation, and testing for C-30 grade concrete. The study compared mixtures made with OPC alone, PPC alone and Partial Replacement of OPC with PPC modified with varying citric acid dosages by weight of PPC.

### 2.2. Materials

Cement: Dangote Ordinary Portland Cement (OPC) and Dangote Portland Pozzolana Cement (PPC) served as binders. OPC was used as the reference cement, whereas PPC partially replaced OPC in blended mixes to evaluate combined performance.

Fine Aggregate: Natural river sand from Alagea was used, conforming to ASTM C33 requirements. Specific gravity, fineness modulus, moisture content, and silt content were measured to verify suitability.

Coarse Aggregate: Crushed basalt aggregates of nominal sizes 9.5 mm (“01”) and 19 mm (“02”) were obtained from Yencomad Crusher. Tests performed included sieve analysis, specific gravity, absorption capacity, bulk density, and aggregate crushing value.

Citric Acid: Commercially available anhydrous citric acid was used as a Type D water-reducing and retarding admixture. Dosages of 0.1 %, 0.2 %, 0.3 %, and 0.4 % (by weight of PPC) were investigated to determine the optimum effect on setting time, workability and strength.

The retarding mechanism of citric acid is primarily attributed to its role as a calcium chelator by forming citrate complexes with calcium ions released during the early stages of hydration; it inhibits the precipitation of calcium hydroxide and slows the dissolution of clinker grains, particularly tricalcium silicate ($C_3S$). This controlled delay allows for improved particle dispersion and water reduction, which can eventually lead to a more refined and compact pore structure in the hardened cement paste. The citric acid dosage used in this study (0.02% by weight of cement) is low and in line with previous studies, which indicate that such small amounts do not significantly alter the pore solution pH or endanger the passivation layer of steel reinforcement. No corrosion was observed during the curing period of the specimens. While this suggests that citric acid is safe at the tested dosage, further long-term studies on reinforced concrete in aggressive environments are recommended to comprehensively evaluate potential corrosion risks.

Water: Potable water conforming to ASTM C1602 was used for both mixing and curing.

### 2.3. Mix Design and Preparation

Concrete was proportioned for C-30 grade with a constant water-cement ratio (W/C) of 0.50, following the Department of Environment (DOE) method. Mix adjustments were made based on the moisture content and absorption capacity of the aggregates to ensure a saturated surface-dry condition. All materials were weighed to the nearest gram. Mechanical mixing was carried out in a pan mixer to achieve homogeneity. The slump test (ASTM C143) was conducted for each batch to evaluate workability.

### 2.4. Casting and Curing

Concrete cubes (100 × 100 × 100 mm) were cast for compressive-strength testing. After 24 hours, specimens were demolded and immersed in clean water at 23 ± 2 °C until the specified testing ages. Each mix was prepared in triplicate to ensure statistical reliability.

### 2.5. Testing Procedures

- Setting Time: Initial and final setting times were determined using a Vicat apparatus (ASTM C191).

- Workability: Measured by standard slump cone test (ASTM C143).
- Compressive Strength: Cubes were tested at 7, 28, and 56 days (ASTM C39). Average values of three specimens were reported for each mix.
- Data Analysis: Comparative analysis was conducted to evaluate the effect of citric acid dosage and PPC replacement on setting time, workability & compressive strength of concrete. The optimum combination was identified based on marginal setting time, compressive strength performance comparable to OPC and improved workability.

*Table 2.1: Designation of Concrete Mixes*

| No. | Mix Code | Concrete samples prepared from |
|---|---|---|
| 1. | $M_O$ | OPC only = ***Reference Mix*** |
| 2. | $M_P$ | PPC only |
| 3. | O-50P-50 | 50% OPC + 50% PPC |
| 4. | O-60P-40 | 60% OPC + 40% PPC |
| 5. | O-70P-30 | 70% OPC + 30% PPC |
| 6. | $M_1$ | 60% OPC + 40% PPC + 0.1%CA (by weight of PPC) |
| 7. | $M_2$ | 60% OPC + 40% PPC + 0.2%CA (by weight of PPC) |
| 8. | $M_3$ | 60% OPC + 40% PPC + 0.3%CA (by weight of PPC) |
| 9. | $M_4$ | 60% OPC + 40% PPC + 0.4%CA (by weight of PPC) |

All compressive strength results were obtained from three replicate specimens and are reported as mean ± standard deviation (SD). One-way analysis of variance (ANOVA) was performed at each curing age (7, 28, and 56 days) to evaluate the statistical significance of differences among OPC, PPC-only, and PPC + citric acid mixes. A significance level of $\alpha = 0.05$ was adopted. When significant differences were detected ($p < 0.05$), post-hoc pairwise comparisons were conducted using Tukey's HSD test to identify the specific groups responsible for variation.

## 3. Theory

The hydration of cement primarily involves the reaction of tricalcium silicate ($C_3S$) and dicalcium silicate ($C_2S$) with water to form calcium silicate hydrate (C–S–H) and calcium hydroxide. In Portland Pozzolana Cement (PPC), pozzolanic materials react with calcium hydroxide to produce additional C–S–H, contributing to long-term strength.

Citric acid, a tricarboxylic organic compound, retards hydration by adsorbing onto cement particle surfaces and forming complexes with calcium ions, thereby delaying the precipitation of hydration products. The retardation effect increases with citric acid concentration but can be balanced to enhance workability without significant loss of strength. This theoretical understanding forms the basis for selecting the dosage range (0.1–0.4%) examined in this study.

## 4. RESULTS AND DISCUSSION

The inclusion of citric acid significantly influenced the setting time and workability of PPC-based concrete. At 0.3% citric acid, the initial and final setting times were extended by approximately 1 hr 50 min and 3 hr 10 min, respectively, compared to the control mix. The slump increased by 55%, indicating enhanced workability and reduced water demand. These results align with the findings of Tinnea and Young (1977a), who reported that organic acids delay the hydration of tricalcium silicate by chelating calcium ions and retarding the formation of calcium silicate hydrate (C–S–H). Compressive strength results showed that PPC alone had lower early-age strength than OPC. However, when combined with 0.3% citric acid, the 28-day compressive strength became comparable to OPC mixes, and the 56-day strength slightly exceeded OPC due to the secondary pozzolanic reaction between calcium hydroxide and reactive silica in PPC (Rajendra, 2013a). Higher citric acid content (0.4%) resulted in excessive retardation and strength loss, consistent with Purnomo et al. (2019a), who observed similar trends in citric-acid-modified concrete. The optimal dosage of 0.3% citric acid was thus identified, balancing extended setting time, improved workability, and satisfactory strength. Furthermore, material

cost analysis revealed that PPC–citric acid mixes offer an economically viable and sustainable option for concrete production in Ethiopia.

### 4.1 Compressive strength of binder compositions

PPC is not intended to fully replace OPC and is already known to delay setting time and affect workability due to its pozzolanic nature, the comparative strength performance at 28 days was prioritized to determine the most balanced mix for further experimental analysis.

In this phase, the 60% OPC + 40% PPC combination—selected based on compressive strength and cost balance—was used to assess the effects of citric acid on workability and setting behavior.

*Table 4.1: 28th day Compressive Strength Results of Binder composition*

| Mix code | Sample No. | Failure load of 100 mm cubes (KN) | Compressive strength of 100mm cubes, (Mpa) | Compressive strength of 150mm cubes, (Mpa) | Standard Deviation SD (MPa) | Standard Error SE(MPa) |
|---|---|---|---|---|---|---|
| O-50P-50 | 1 | 347 | 24.8 | 23.8 | | |
| | 2 | 372 | 26.3 | 25.2 | | |
| | 3 | 342 | 28.6 | 27.5 | | |
| | **Average** | | **26.6** | **25.5** | **1.87** | **1.08** |
| O-60P-40 | 1 | 269 | 27.5 | 26.4 | | |
| | 2 | 244 | 28.8 | 27.6 | | |
| | 3 | 235 | 25.1 | 24.09 | | |
| | **Average** | | **27.1** | **26.03** | **1.78** | **1.03** |
| O-70P-30 | 1 | 269 | 27.6 | 26.5 | | |
| | 2 | 301 | 30.5 | 29.3 | | |
| | 3 | 257 | 26.9 | 25.8 | | |
| | **Average** | | **28.3** | **27.2** | **1.85** | **1.07** |

The mix with 70% OPC and 30% PPC demonstrated the highest compressive strength (27.2 MPa), as expected, due to the higher content of clinker, which accelerates hydration and strength gain (ACI Committee 233, 2003). However, the marginal difference between this mix and the 60% OPC + 40% PPC mix (only 1.17 MPa) suggests that the latter provides a more favorable balance between strength and potential cost or environmental impact (Bijen, 1996). On the other hand, the 50%

OPC + 50% PPC combination showed the lowest strength (25.5 MPa), reinforcing the limitation of using high PPC proportions when early or design strength is a primary concern (Hewlett & Liska, 2019).

The 40% PPC replacement level was selected as the base binder composition following preliminary tests of 30%, 40%, and 50% replacement. The 60% OPC + 40% PPC mix was chosen because it provided the most optimal balance between target compressive strength (reaching 26.03 MPa at 28 days) and the economic benefit of reducing OPC content.

Overall, while all three mixes achieved satisfactory strength values for general structural applications, the 60% OPC + 40% PPC mix was found to be an optimal compromise between mechanical performance and material efficiency, justifying its selection for subsequent experimental phases involving admixture modification.

### 4.2. Setting Time

*Table 4.2: Effect of citric acid on the initial & final setting time*

| Mix code | Mix Type | Delay in setting time relative to reference mix (hrs. : min) | |
|---|---|---|---|
| | | Initial | Final |
| $M_1$ | 60%OPC + 40%PPC + 0.1% CA (by weight of PPC) | 1:30 | 2:40 |
| $M_2$ | 60%OPC + 40%PPC + 0.2% CA (by weight of PPC) | 1:35 | 2:55 |
| $M_3$ | 60%OPC + 40%PPC + 0.3% CA (by weight of PPC) | 1:50 | 3:10 |
| $M_4$ | 60%OPC + 40%PPC + 0.4% CA (by weight of PPC) | 1:55 | 3:50 |

According to ASTM-C494 (2003), the delay in initial and final setting time must not be less than (1) hour and not more than (3:30) hours relative to reference mix, respectively. It can be observed that the 0.1, 0.2 & 0.3% dosage of citric acid causes a delay in initial and final setting time within ASTM-C494 (2003) range. However the result of 0.4% is not conforming to ASTM-C494 (2003) requirements.

The citric acid dosage range of 0.1% to 0.4% was established through trial experiments; it was observed that dosages exceeding 0.4% resulted in setting time delays that failed to comply with ASTM C494 standards and began to adversely affect strength development. The range was determined through trial experiments. We found that 0.4% was the maximum effective dosage, as any higher amount caused setting time delays that exceeded the ASTM C494 limits (not more than 3:30 hours relative to the reference mix) and began to negatively impact strength.

Citric acid retards concrete setting by chelating calcium ions, slowing the hydration of key cement compounds ($C_3A$ and $C_3S$). This effect is dosage-dependent, with higher concentrations causing longer delays in initial and final setting times. In this study, the maximum dosage was limited to 0.4% of PPC cement, as higher amounts exceeded ASTM C494 limits and could negatively affect workability and compressive strength. The 0.4% dosage was chosen to balance extended workability with acceptable setting and strength performance.

### 4.3. Workability

Workability, as measured by the slump test, is an essential property that determines how easily concrete can be mixed, placed, and compacted.

*Table 4.3: Slump test results*

| Mix code | Mix Type | Slump length (mm) |
|---|---|---|
| $M_O$ | OPC Mix | 55 |
| $M_P$ | PPC Mix | 60 |
| $M_1$ | 60% OPC + 40% PPC + 0.1% CA | 65 |
| $M_2$ | 60% OPC + 40% PPC + 0.2% CA | 70 |
| $M_3$ | 60% OPC + 40% PPC + 0.3% CA | 85 |
| $M_4$ | 60% OPC + 40% PPC + 0.4% CA | 95 |

The addition of citric acid slightly improved the workability of concrete mixes compared to the control, due to its plasticizing effect and ability to adsorb onto cement particles, reducing interparticle friction and increasing free water for lubrication. Combined with Portland Pozzolana Cement (PPC), which enhances flow through its finer particles and pozzolanic content, citric acid further improves fresh concrete properties. This synergistic effect suggests that careful dosing of citric acid can enhance workability without compromising other key properties.

The incorporation of citric acid significantly enhanced the workability of PPC-based concrete. Compared with the control OPC mix (55 mm slump), the mix containing 0.3% citric acid achieved a slump of 85 mm, representing approximately a 55% increase. This improvement is attributed to the chelation of $Ca^{2+}$ ions by citric acid, which delays early hydration and reduces flocculation of cement particles. The adsorption of citrate ions on cement grain surfaces increases electrostatic repulsion and particle dispersion, thereby releasing entrapped water and improving flowability.

In addition, the finer particle size of PPC contributes to improved packing density and lubrication effects in the fresh mix. However, at higher dosage (0.4%), although slump increased to 95 mm, excessive retardation may interfere with early hydration product formation, potentially affecting early-age strength. These findings are consistent with Tinnea and Young (1977), who reported that organic acids improve dispersion by suppressing rapid $C_3A$ hydration.

The statistical variability (SD < 5% of mean) confirms that the observed improvement in workability is systematic rather than experimental fluctuation.

### 4.4. Compressive Strength

The compressive strength of concrete is one of the most critical factors in determining its suitability for reinforced concrete applications. Compressive strength was measured at 7, 28 and 56 days of curing. Compressive strength tests were done for the C-30 concrete class. Molds measuring 100 mm in cubes were used for the compressive strength tests. Neville, “Properties of Concrete”, 4th edition, suggests a conversion factor of 0.96 to translate 100mm cube strength to 150mm cube strength.

*Table 4.4: Compressive Strength Results*

| No. | Mix Code | 28th day Average Compressive Strength Result (Mpa.) | Standard Deviation SD (MPa) | Standard Error SE(MPa) |
|---|---|---|---|---|
| 1. | $M_O$ | 33.9 | 1.55 | 0.89 |
| 2. | $M_P$ | 20.9 | 1.11 | 0.64 |
| 3. | $M_1$ | 26.5 | 2.18 | 1.26 |
| 4. | $M_2$ | 28.2 | 1.76 | 1.02 |
| 5. | $M_3$ | 32.4 | 1.77 | 1.02 |
| 6. | $M_4$ | 30.1 | 1.72 | 0.99 |

The concrete mixed with 40% PPC and 0.3% citric acid (by weight of PPC) has a compressive strength of 32.4 for C-30 at 28 days, which is comparable with OPC, based concrete. Therefore, the preconditions listed in ACI 301 for acceptance of compressive strength of concrete are likewise satisfied by the compressive strengths of concrete prepared with 40% PPC and 0.3% citric acid (by weight of PPC) at 28 days.

The mix with 40% PPC and 0.3% citric

acid achieved compressive strength slightly lower than the control, mainly due to the dilution effect of PPC and the retarding action of citric acid on cement hydration. While citric acid improves workability, excessive amounts can delay the formation of strength-giving compounds, so a maximum dosage of 0.4% was adopted to balance setting time and compressive strength.

The compressive strength development of PPC–citric acid concrete reflects the combined influence of dilution, retardation, and secondary pozzolanic reactions. At early ages, mixes containing citric acid exhibited slightly reduced strength due to delayed hydration of tricalcium silicate ($C_3S$), as citrate complexes temporarily inhibit calcium hydroxide precipitation. This prolongs the induction period of hydration and slows the formation of primary C–S–H gel.

However, at 28 days, the mix containing 40% PPC and 0.3% citric acid achieved 32.4 MPa, approaching the control OPC strength (33.9 MPa). The later-age strength recovery is attributed to the pozzolanic reaction between reactive silica in PPC and calcium hydroxide, forming additional secondary C–S–H gel. This reaction refines pore structure and improves matrix densification.

At 56 days, strength slightly exceeded that of PPC-only mixes, confirming that moderate retardation does not permanently hinder hydration but rather redistributes it over time. In contrast, the 0.4% dosage produced marginal strength reduction due to excessive complexation of calcium ions, which can inhibit normal crystal growth of hydration products.

One-way ANOVA analysis ($p < 0.05$) confirms that the differences between control, PPC-only, and PPC + citric acid mixes are statistically significant, indicating that the combined PPC–citric acid interaction has a measurable influence on compressive strength development.

The ANOVA results confirmed statistically significant differences among the mixes at 28 days ($p < 0.05$). The effect size indicates that citric acid dosage significantly influences strength development. Post-hoc analysis showed that the 0.3% citric acid mix did not differ significantly from the control OPC mix ($p > 0.05$), whereas the PPC-only and 0.4% mixes exhibited statistically lower strength ($p < 0.05$). This confirms that 0.3% represents an optimal dosage balancing retardation and strength performance.

### 4.5. Cost Comparison

The cost comparison is done between the concrete mixes created with OPC, and the concrete mixes prepared with 40% PPC and 0.3% Citric acid. The cost of the concrete mix made with 40% PPC and 0.3% citric acid is 258.856 Ethiopian birr less per cubic meter for C-30 than the mix made with OPC. This indicates that cost savings can be obtained without affecting the required compressive strength by employing concrete mix prepared with PPC and citric acid.

Concrete's widespread use makes cost savings per cubic meter highly impactful, especially in large projects. This study's experimental mix achieved economic efficiency by partially replacing OPC with the less expensive PPC and using citric acid to improve workability, reducing the need for additional costly admixtures while maintaining technical performance.

Although this study does not include advanced microstructural (e.g., SEM, XRD) or durability investigations, its originality lies in the systematic experimental evaluation of the combined effect of PPC and citric acid on the compressive strength of reinforced concrete under varying mix designs. Previous research has implemented detailed microstructural analyses such as XRD and SEM to examine the influence of citric acid on cement hydration mechanisms and phase evolution in cementitious systems, as well as durability-oriented studies on citric acid modified concrete compositions. Additionally, other researchers have examined microstructural and durability characteristics of blended or admixed cementitious composites with different admixtures and SCMs. However, comprehensive microstructural and durability

*Table 4.5: Cost Comparison*

| Ingredients | Unit | Price (birr / unit) | $M_0$ (OPC only) | | $M_{0.3}$ (60% OPC + 40% PPC = 0.3%CA) | |
|---|---|---|---|---|---|---|
| | | | Quantity (Qt.) | Cost (birr) | Quantity (Qt.) | Cost (birr) |
| Cement (Dangote-PPC) | Qt. | 1300 | | | 1.51544 | 1970.072 |
| Cement (Dangote-OPC) | Qt. | 1650 | 3.8 | 6270 | 2.28 | 3762 |
| Citric Acid | Kg. | 612 | | | 0.456 | 279.072 |
| Sum | | | | 6270 | | 6011.144 |
| Cost Difference | | | | 258.856 birr | | |

characterization in the specific context of citric acid combined with locally produced Ethiopian PPC is beyond the scope of the present work and is therefore not addressed here. This study instead provides valuable quantitative data for practitioners and researchers aiming to optimize concrete mixes using PPC and citric acid, thereby filling a practical knowledge gap in concrete mix design.

## 5. CONCLUSIONS AND FUTURE WORK

The combined utilization of Portland Pozzolana Cement (PPC) and citric acid as a water-reducing and retarding admixture demonstrates a promising approach for producing sustainable, economical, and high-performance reinforced concrete. The experimental findings indicate that incorporating citric acid at an optimal dosage of 0.3% by weight of PPC significantly enhances the workability of fresh concrete while maintaining an acceptable setting time and achieving compressive strength levels comparable to those of mixes prepared with Ordinary Portland Cement (OPC). This balance between workability and strength performance makes the PPC–citric acid blend a viable alternative to conventional OPC systems.

Furthermore, the study underscores the practical relevance of PPC–citric acid concrete for structural applications, particularly in warm climatic regions such as Ethiopia, where extended setting time can improve handling, placement, and finishing operations. The integration of a natural, eco-friendly additive like citric acid also contributes to sustainability by promoting reduced cement consumption and minimizing the reliance on synthetic chemical admixtures.

To build upon these findings, future research should focus on examining the long-term hydration mechanisms of citric-acid-modified PPC concrete. In particular, studies should investigate its compatibility with other chemical and mineral admixtures, as well as its influence on key durability parameters, including drying shrinkage, thermal performance, and reinforcement corrosion resistance under diverse environmental conditions. Such investigations will provide deeper insights into its long-term performance and broaden its potential for use in sustainable structural concrete applications.

This study is limited to the experimental evaluation of compressive strength, setting time, and workability of C-30 grade concrete with a fixed water–cement ratio of 0.50 under

controlled laboratory curing conditions. Other important mechanical properties such as tensile and flexural strength were not investigated.

In addition, advanced durability assessments (e.g., sulfate resistance, chloride penetration, shrinkage, and creep) and microstructural analyses (e.g., SEM, XRD, or thermal analysis) were beyond the scope of this research due to time constraints and because several of these properties have been extensively examined by other researchers. The dosage range of citric acid was restricted to 0.1%–0.4% by weight of PPC, and strength development was monitored up to 56 days only. Furthermore, the findings are based on specific locally sourced materials and laboratory-scale specimens; therefore, full-scale structural behavior and long-term field performance were not evaluated.

All concrete specimens, including control OPC, PPC, and PPC + citric acid mixes, were cast and cured under identical conditions. The standard curing temperature is specified within a defined range, and this was maintained using appropriate environmental control mechanisms to ensure stable curing conditions. Accordingly, samples were kept in a controlled curing room at 23 ± 2 °C and 95% relative humidity until testing.Maintaining consistent environmental conditions was particularly important due to the temperature sensitivity of citric acid, which can influence hydration kinetics and setting time. This approach ensures that any observed differences in compressive strength are attributable to variations in mix composition rather than environmental variability.

## REFERENCES


1. ACI Committee 233. (2003). Slag cement in concrete and mortar (ACI 233R-03). American Concrete Institute.
2. ACI Committee 301. (2016). Specifications for structural concrete (ACI 301-16). American Concrete Institute.
3. Addisu, F. (2014). Study on the uses of Derba Ordinary Portland and Portland Pozzolana cements for structural concrete production. Addis Ababa University.
4. Albadrani, M. A. (2025). Long-term performance of Portland pozzolana cement blended with rice husk ash in sustainable concrete production. Construction and Building Materials, 412, 134512.
5. ASTM C33/C33M-18. (2018). Standard specification for concrete aggregates. ASTM International.
6. ASTM C39/C39M-20. (2020). Standard test method for compressive strength of cylindrical concrete specimens. ASTM International.
7. ASTM C143/C143M-15a. (2015). Standard test method for slump of hydraulic-cement concrete. ASTM International.
8. ASTM C1602/C1602M-18. (2018). Standard specification for mixing water used in the production of hydraulic cement concrete. ASTM International.
9. ASTM C191-19. (2019). Standard test methods for time of setting of hydraulic cement by Vicat needle. ASTM International.
10. ASTM C494/C494M-19. (2019). Standard specification for chemical admixtures for concrete. ASTM International.
11. Bijen, J. (1996). Benefits of slag and fly ash. Construction and Building Materials, 10(5), 309–314.
12. Ciacchella, M., Rossi, F., Bianchi, A., & Conti, L. (2025). Citric acid as a salt crystallization inhibitor in cement-based materials under wet–dry cycling. Materials and Structures, 58(3), 102.
13. Department of Environment (DOE). (1988). Design of normal concrete mixes (2nd ed.). Building Research Establishment.
14. Dhanya Sathyan, D. (2018). Influence of chemical admixtures on the strength and durability of pozzolanic concrete. Construction and Building Materials, 173, 631–640.
15. Hewlett, P. C., & Liska, M. (2019). Lea's chemistry of cement and concrete (5th ed.). Butterworth-Heinemann.
16. Neville, A. M. (2011). Properties of concrete (5th ed.). Pearson Education.

17. Nigus, A. (2005). A comparative study of Ordinary Portland Cement (OPC) and Portland Pozzolana Cement (PPC) with emphasis on their strength and durability. Addis Ababa University Institutional Repository.
18. Purnomo, E., Dewi, R. S., & Setiawan, D. (2019a). Influence of citric acid on the setting time and strength of Portland cement. IOP Conference Series: Materials Science and Engineering, 669, 012025.
19. Purnomo, S., Sumarni, I. N., & Saputro, I. (2019b). Effect of citric acid concentration on compressive strength of concrete bricks. Journal of Materials in Civil Engineering.
20. Qin, Y., Zhang, H., Liu, X., & Wang, J. (2024). Effect of citric acid–modified chitosan on hydration kinetics, strength development, and shrinkage behavior of cementitious systems. Cement and Concrete Composites, 146, 105321.
21. Rajendra, K. (2013a). Performance of fly ash in Portland Pozzolana Cement. International Journal of Civil Engineering Research, 4(2), 143–152.
22. Rajendra, P. (2013b). Study on the performance of Portland pozzolana cement in structural applications. International Journal of Civil and Structural Engineering, 4(2), 85–92.
23. Tinnea, J., & Young, J. F. (1977a). Effect of citric acid on the hydration of Portland cement. Cement and Concrete Research, 7(1), 37–45.
24. Tinnea, J., & Young, J. F. (1977b). Retardation of cement hydration by organic admixtures. Cement and Concrete Research, 7(3), 373–383.

# Investigating the possibility of producing Polyhydroxyalkanoates (PHAs) Using Hydrolysates of Napier grass by Burkholderia Sacchari strain

**Adane Bazezew Shiferaw[1*] and Sintayehu Nibret Tiruneh[1*]**

[1]School of Chemical and Bio Engineering, Collage of Technology and Built Environment, Addis Ababa University, P.O.B 385|Addis Ababa | Ethiopia

*Corresponding Authors: A. B. Shiferaw (adane.bazezew@aau.edu.et)
S. N. Tiruneh (sintayehu.nibret@aau.edu.et)

**Abstract**

Bacteria produces Polyhydroxyalkanoates (PHAs), which are macromolecules. They are inclusion bodies that build up as reserve resources while bacteria grow under various stress situations. PHAs have been chosen as alternatives for the development of biodegradable polymers due to their rapid degradability under natural environmental circumstances. This study aimed to produce reducing sugars from Napier grass for use as a carbon source in polyhydroxyalkanoate (PHA) synthesis. The effects of temperature, pH, and culture time on growth yields were adjusted using Response Surface Methodology using a Box-Behnken design.

Burkholderia Sacchari strain was chosen from more than 300 bacterial strains capable of PHA accumulating strains based on its ability to consume both hexose and pentose sugars and has a capacity of accumulating high mass PHA granules inside its cells. At 200 rpm, optimal pH, fermentation temperature, and incubation time for the isolate to produce the highest PHA were 7, 35 °C, and 48 hour, respectively.

When hydrolysates of Napier grass was employed as carbon sources and ammonium sulphate as nitrogen sources, the strain was able to collect 62.1% PHA from its total biomass. The extracted PHAs' FTIR spectra show strong peaks at wavenumbers that are unique to PHAs as C–H, $CH_2$, O-H, C=O, and C–O groups. The extract's resemblance appropriateness for bioplastic production were validated by UV–Vis spectrophotometric analysis.

**Keywords:** Polyhydroxyalkanoate, Napier grass, Glucose-rich hydrolysate, PHA productivity, Burkholderia Sacchari

## 1. Introduction

With an ever-growing world population, climate change, globalization and industrialization; have intensified the uncontrollable and rapid use of non-renewable energy sources such as fossil fuels and minerals as planet earth is losing its natural resources (Muhammadi et al., 2015). While the growing environmental problem has many sources, the most common organizations directly or indirectly involved are synthetic polymers, in particular plastics. Petrochemical plastics such as polyethylene terephthalate (PET), polyvinylchloride (PVC), polyethylene (PE), polypropylene (PP), polystyrene (PS) and polyamide (PA) have been commonly used as packaging materials. However, due to the high demand for their use for many purposes (low cost, durability and functional advantages), improper discarding, and environmental persistence, their use has actually been cut due to their low biodegradability, which causes significant environmental problems ( Marsh & Bugusu, 2007). In view of rising energy demand and the decrease of fossil resources, the global economy is currently trying to replace recognized energy sources with greener, bio-based and renewable alternatives (Bhatia et al.,

2019; Venkata Mohan et al., 2016).

Environmental, health, and political concerns, as well as the aforementioned problems, motivated the development of bioplastics such as Polyhydroxyalkanoates (PHAs); polyesters produced during the secondary metabolism of bacteria and
archaea in the presence of excess carbon sources and insufficiency of nutrients inside the cell's cytoplasm, allowing for a lower environmental impact (Laycock et al., 2014). In the PHAs group, polyhydroxybutyrate (PHB) is gaining enormous consideration due to its extraordinary characteristics, such as a higher degree of crystallinity, tensile strength, and melting temperature (175 $^{o}$C) with low permeability for $H_2O$,$O_2$, and $CO_2$ (Saratale et al., 2020).

The major challenge for industrial production of PHA is the reliable and scalable supply of carbon sources, as it makes up to 48-50% of PHA production costs (George et al., 2020; Pradhan et al., 2017). Recently, great work has been devoted to lowering the cost of PHA production by employing strategies such as establishing efficient bacterial strains, optimizing fermentation and recovery processes, and so on. So producing PHAs using cheap carbon source would reduce the production cost. According to Bugnicourt et al. biodegradable bio plastics are basically divided in to thee groups according to their sources: biomass based (Proteins, Lipids, and Polysaccharide), microorganism based (PHA) and biotechnology based (Polyactides and Polylacticacid) (De Donno Novelli et al., 2021). In sustainable PHA production using non-edible, industrial and agricultural wastes, abundant and renewable carbon sources such as waste biomass are used. This will not only ensure agreement with zero waste policies but also enable upcycling of the generated wastes within bio refineries to high value products (Radhika & Murugesan, 2012; Sayyed et al., 2021). Cost optimization production process will be done by using waste materials (cheap carbon sources), recombinant strains techniques and use of mixed microbia l culture (MMC) with open systems that do not require sterile conditions, coupled to that of wastes or surplus based feeds (Jong Il Choi & Lee, 1997; Ienczak et al., 2013).

Because of its high availability and low cost worldwide, lignocellulosic biomass, which mainly consists of cellulose, hemicellulose, and lignin as main component, has recently received increased attention as a promising sustainable and carbon-neutral feedstock for the development of biofuels and platform chemicals (Bhatia et al., 2019). For instance, polysaccharides can be hydrolyzed by using different chemical, physical, enzymatic or combination of those methods from cellulose and hemicellulose, followed by biotransformation into different biofuels such as bioethanol, hydrogen, biodiesel, paper, lumber and bioplastics.

Napier grass is one type of lignocellulosic material that contains cellulose, hemicellulose and lignin as main alignment and has $C_4$ metabolism (Basso et al., 2014; Lu et al., 2019). It is a potential feedstock for production of biofuel like biogas (Rodriguez et al., 2017), bioethanol (Ohimain, 2014) and bio butanol (He et al., 2017) as it has strong adaptableness, high growth rate, high biomass yield, drought resistance and wide availability properties. In order to extract monosaccharides from Napier grass, different pretreatment methods are being investigated by different researchers. Cellulose ethanol derived from Napier grass has been extensively studied by Yasuda et al by using Low-Moisture Anhydrous Ammonia (LMAA) Pretreatment combined with enzymatic hydrolysis of Napier grass to obtain a total sugar yield of 0.35 g- sugar per g-biomass, ethanol yield of 74.1% by using Escherichia coli (Yasuda et al., 2014). Napier grass has been also converted to butanol by pretreatment, enzymatic hydrolysis and ABE fermentation (He et al., 2017).

In this study, Napier grass was chosen for carbon source and undergoes with NaOH pretreatment and enzyme hydrolysis to extract monosaccharides to produce PHA. To the best

of the author's knowledge, this is the first study to explore the use of Napier grass as a feedstock to produce PHA.

## 2. Materials and Methods

### 2.1 Material

The raw material, mature stems of Napier grass (Pennisetum purpureum), was obtained from Menagesha Mushroom Farm in Ethiopia. The fresh biomass was milled first, then sun-dried for two weeks to reduce moisture content considerably. Once suitably cured, the material was manually cut into small segments of 1-2 cm length with scissors and hand cutters. The chopped grass was further refined by passing it through a mechanical cutting mill, which produced fine, consistent particle sizes. The material was categorized by running it through a standard 150 µm sieve to ensure homogeneity for future use.


*Figure 2.1: Napier grass Processing*

### 2.2. Methodology

Figure 2.2 depicts the overall experimental methodology, which consists of four sequential stages: (1) producing glucose from Napier grass, (2) inoculating, propagating, and fermenting using that glucose, (3) extracting and purifying the synthesized PHA, and (4) characterizing the final PHA product.

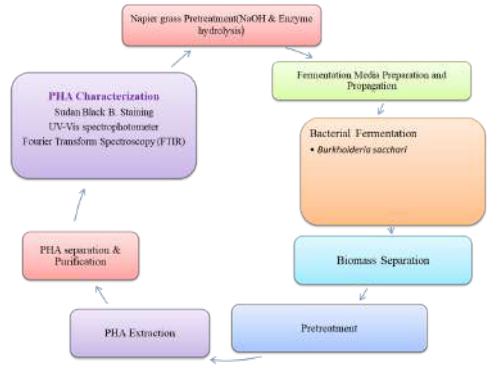


*Figure 2.2: Major Steps in PHA Production Process*

#### 2.2.1 Alkaline Hydrolysis

In a sealed Erlenmeyer flask, 50 g of the Napier grass sample was submerged in 300 mL of 2 % (w/v) NaOH (a solid to liquid ratio of 1:6). The NaOH pretreatment bottles were autoclaved at 121 $^{o}$C for 1 hour. After that, they were allowed to cool to ambient temperature (Phitsuwan et al., 2016). Following the pretreatments, each pretreated solid was separated from the liquid fraction using a filter. The solid portions were rinsed in distilled water until their pH was neutral. Following filtering, the solid residue was dried for at least 48 hours in a hot-air oven at 80 oC before being kept in a sealed plastic bag at room temperature for later enzymatic hydrolysis.

#### 2.2.2. Enzymatic Hydrolysis

Enzyme hydrolysis was done according to Kongkeitkajorn et al (Kongkeitkajorn et al., 2020; Pensri et al., 2016) methods. Multi component Cellulase (Novozymes, Denmark) was used to hydrolyze pretreated grasses. In a 500-mL laboratory container, 100 mL of 50 mM citrate buffer solution (pH 5.0) was mixed with the pretreated grass with loading of 15 %( W/V). After that, the enzyme was added at a loading volume of 2 ml/g substrate and combined, and the mixture was incubated in a water bath at 50 oC with continual mixing for 72 hour with shaking at 150 rpm. 0.5 g/L sodium azide was added to the process to avoid microbiological contamination. By boiling the contents for 5 minutes, the hydrolysis reaction

was halted. After all samples are withdrawn, the hydrolysate was centrifuged for 15 minutes at 4 oC and 4000 rpm, and the supernatant was tested for total reducing sugar using the DNS method.

### 2.2.3. Inoculation

In this investigation, Burkholderia sacchari, which was recently reclassified as Paraburkholderia sacchari, brought from Switzerland, was utilized. To grow the organism, Luria Bertani broth (NaCl, 5 g/L; Tryptone, 10 g/L; and yeast extract, 5 g/L) was employed. In a 500 mL shake flask, 100 mL of media was inoculated with one overnight culture from an agar slant. The bacterial isolates were incubated for 24 hours at 30 oc and 150 rpm (Oliveira-Filho et al., 2020). After 24 hours, the entire 50-mL culture was transferred aseptically to a fresh 250-mL LB broth culture (total 300 mL; enclosed in a 500-mL Erlenmeyer flask) and cultured as previously described.

### 2.2.4. Fermentation Media Preparation, Propagation and Fermentation

The following mineral salts media (MM) composition was modified to restrict nitrogen availability (in g/L): KH2PO4, 9.0; $Na_2HPO_4$ $2H_2O$, 3.0; $(NH_4)_2SO_4$, 2.0; $MgSO_4 \cdot 7H2O$0.2 g; $CaCl_2 \cdot 2H_2O$, 0.02,; (NH4)5Fe(C6H4O7)2, 0.03 and trace elements solution (2 mL/L) (de Sousa Dias et al., 2017). The media was made in bulk and then distributed evenly across the test flasks in accordance with the protocols devised for maximum growth. This prior culture was applied as an inoculum to mineral salts media (10% v/v) (Penkhrue et al., 2020). Separate autoclaves were used for the MgSO47H2O, $CaCl_2$, $2H_2O$, Hydrolysates and (NH4)5Fe(C6H4O7)2 solutions were added to the medium aseptically. Glucose rich hydrolysates were added 5(%W/V). pH was adjusted to the experimental run by adding NaOH (5M) or $H_2SO_4$ (5M) and 200 rpm in a shake incubator.

### 2.2.5. Measurement of Dry Biomass

Dry biomass is measured by taking samples (10 mL) from the culture media at set intervals and centrifuging them at 8000 rpm for 15 minutes. Remove supernatant and collect pellet at the bottom by rinsing with distilled water. The pellets were dried at 70°C, and weighed in an analytical scale to constant weight. The pellet samples are kept at room temperature in a dry place until PHA extraction is performed (Acosta-Cárdenas et al., 2018).

### 2.2.6. PHA Extraction

Solvent extraction followed by non-solvent precipitation was employed to recover (Kunasundari & Sudesh, 2011). Following that, the lyophilized cells were placed in a conical flask with 100 mL sodium hypochlorite (5%) and 100 mL chloroform. For 12 hours, the mixture was stirred in a rotary shaker at 200 rpm and 30 °C. The suspension was placed in a separating funnel and allowed to stand for 30 minutes to allow the three phases to separate: an upper phase containing hypochlorite solution, a middle phase containing non-PHA material and a bottom phase containing PHA solubilized in chloroform. To precipitate the PHAs, the bottom phase was decanted into a beaker and nine parts methanol were added. Finally, the PHA-precipitate was dried at 30 °C by evaporation, yielding white flakes or powder (Singh et al., 2021).

### 2.2.7. Determination of Total Reducing Sugar using DNS Method

In the manual approach, 30 ml of modified DNS reagent was added to 10 ml of sample plus 10 ml of distilled water in a test tube, which was then heated in a boiling water bath for 15 minutes and chilled for at least 15 minutes. The absorbance was then measured at 540 nm. Several modifications in sample volume and wavelengths were investigated. Glucose standard curves were developed ( Miller, 1959).

### 2.3. Characterization

#### 2.3.1. Screening by Sudan Black B. Stain

After PHA production was established, ten milliliters of media were centrifuged at 6000 rpm for 20 minutes and Sudan staining was performed to confirm PHA production. A smear of 72 hour old strains was stained for 15 minutes with 0.3 percent (w/v) Sudan Black B. solution, then distaining with alcohol (50 percent v/v) and counterstaining with safranin solution (0.5 percent, w/v) ( Sayyed et al., 2021).

#### 2.3.2. UV–Vis Spectrophotometer Analysis of PHA

The extracted PHA was dissolved in chloroform and scanned in the range of 200–320 nm against a chloroform blank a Perkin-Elmer Lambda 950 UV/VIS spectrometer, with the spectrum evaluated for a strong peak at 240 nm (Selvakumar et al., 2011).

#### 2.3.3. FTIR spectrophotometer analysis of PHA

PHA was validated using FTIR spectroscopy after 1 mg of sample and 10mg of spectral pure anhydrous potassium bromide crystals were crushed thoroughly and formed into a pellet and relative intensity of transmitting light energy was evaluated against the wavelength of absorption 4000–400 cm-1(Radhika & Murugesan, 2012).

3. Results and Discussion

3.1. Benedicts' Test

The benedict test indicates that the color of the hydrolysate was changed to brick red after it was mixed with benedict solution and heated for 5 minutes and the color changes to brick red as it was shown from figure 4.1, signifies the solution has more than 2% of reducible sugar (Aryal, 2019.) Benedict's reagent comprises blue copper (II) sulfate (CuSO4)5H2O, which is reduced to red copper (I) oxide by aldehydes, resulting in carboxylic acids being formed. Copper oxide is water insoluble and thus precipitates. Depending on how many copper (II) ions are present, the color of the final solution can range from green to brick red (Benedict, 1911; Pataca et al., 2007). Color change to bricks red indicates the pretreated Napier grass using NaOH and Cellulase enzyme hydrolysis produces significant amount of reducible sugars that can be used as a feedstock for fermentation process.

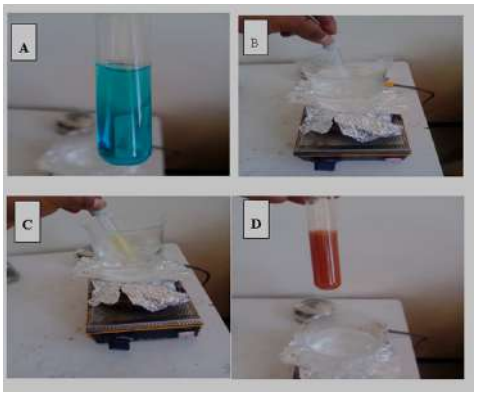


*Figure 3.1: The Benedict Test of the Produced Reducible Sugar*

### 3.2. Total Reducing Sugar Analysis of the Hydrolysates

The DNS approach was used to estimate sugar reduction (Miller, 1959). To estimate the total reducing sugar after alkaline pretreatment and enzymatic hydrolysis, a standard curve was performed by the DNS technique. The sample absorbance at 540nm was computed from the calibrated data, and the total reducing sugar content was determined to be 28.74 g L-1. In this study, 3.2 g of sugar was recovered, which is less than a previous study that yielded 3.9 g of sugar from a 5 g sample load (He et al., 2017). This indicates from Napier grass, high amount of reducible sugars were produced using NaOH and Cellulase enzyme, is a potential candidate for PHA production. Higher quantities of fermentable sugars in the hydrolysate are preferred for fermentation to generate higher PHA concentrations. The major cause of this disparity is the age during cultivation and kind of Napier grass used for this investigation.

### 3.3. Sudan Black B. Staining

Sudan Black B staining was used to detect PHA buildup within the bacterial isolate. This technique distinguishes PHA-producing cells by coloring the intracellular polymer granules with a distinctive blue-black color. The data, shown in Figure 3.2, show a considerable favorable response. A quantitative study of the stained slide revealed that revealed that approximately two-thirds of the total cell count exhibited positive staining.

This high frequency of accumulation, consistent with (Jong-il Choi & Lee, 1999). Findings, demonstrates that PHA biosynthesis is resilient and efficient under the test conditions.

This approach takes advantage of the Sudan Black B dye's lipophilic properties, which have a high affinity for the hydrophobic surfaces of intracellular PHA granules. When applied to fixed cell cultures put on glass slides, the dye preferentially enters the cell wall and membrane and binds to the lipid inclusions. This interaction produces a strong visual difference under bright-field microscopy: PHA-accumulating cells have a pronounced blue-black coloration, whereas non-producer cells are unstained or have a weak, counterstained hue.

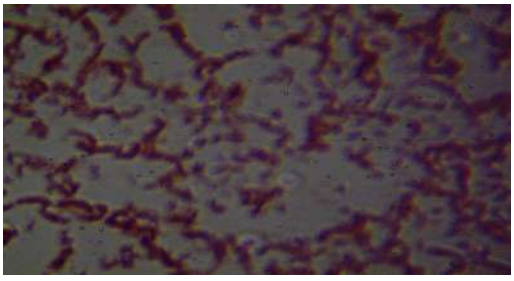

*Figure 3.2: Microscopic Image of PHA Granules by Sudan Black B. Staining*

### 3.4. UV-Vis Spectrophotometer Analysis of PHA

In this study, chloroform was chosen as the solvent blank because of its well-documented efficacy as a superior solvent for a wide range of polymeric compounds, including plastics and, more specifically, Polyhydroxyalkanoates (PHA) (Kourilova et al., 2023 ). Its application is crucial in ultraviolet-visible (UV-Vis) spectrophotometry because it offers a baseline absorbance profile against which the analytes individual absorbance may be correctly measured. The presence and content of PHA in the extracted samples were next assessed by measuring their absorbance patterns across the UV spectrum, from 200 to 320 nm, as shown in Figure 3.3.

This quantitative analysis is based on the Beer-Lambert equation, which states that the absorbance of a solution is directly proportional to the concentration of the absorbing species inside it. As a result, a higher measured absorbance at a specific wavelength correlates directly with a larger concentration of PHA in the chloroform solution (Skoog et al., 2018).

The obtained spectra indicated a prominent and sharp absorption peak at wavelength 240 nm. This spectral characteristic is recognized as a fingerprint for PHA polymers because the polymer's molecular links absorb light strongly at this energy level. The existence of this distinctive peak, rather than a flat or featureless baseline, provides strong confirmation of both PHA granule formation and effective extraction from the bacterial sample. This conclusion is consistent with recognized spectroscopic techniques for PHA identification, as demonstrated by Ranganathan et al., 2022. The sharpness of the peak indicates a relatively clean extract with little contamination from other biological components that may absorb at different wavelengths (Ranganathan et al., 2022)

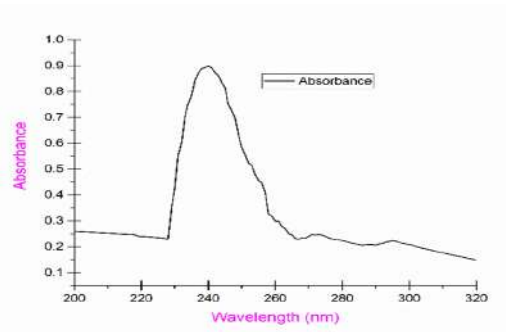


*Figure.3.3: UV- Vis Spectroscopy of PHA*

### 3.5. FTIR Spectrophotometer Analysis of PHA

Fourier Transform Infrared (FTIR) spectroscopy was used to analyze the functional groups of the polyhydroxyalkanoate (PHA) biopolymer derived from Burkholderia Sacchari. This analytical approach is based on the idea that when exposed to infrared radiation, chemical bonds inside a molecule vibrate at specific frequencies, resulting in a distinct absorbance spectrum that serves as a molecular "fingerprint" for the material. Figure 3.4 depicts the resulting spectrum for the retrieved PHA, and the key aspects are discussed in depth below (Atifah et al., 2001).

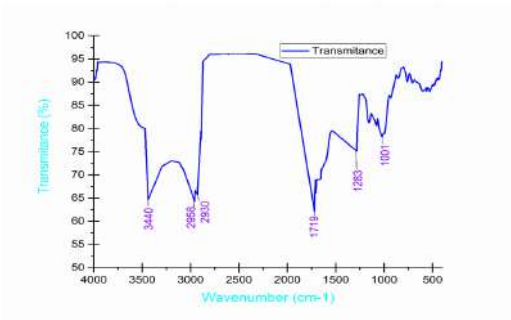


*Figure 3.4: FTIR Spectra of the Extracted PHA*

The spectral analysis of the PHA polymer revealed complex absorption patterns indicative of its intricate structure. Notably, a broad absorption band around 3440 $cm^{-1}$ correlates with O-H stretching vibrations, signaling terminal hydroxyl groups that can form strong intermolecular hydrogen bonds. Additionally, distinct peaks in the high-frequency range of 2800 to 3000 $cm^{-1}$ are attributed to aliphatic C-H stretching, with specific peaks at 2930 $cm^{-1}$ and 2958 $cm^{-1}$ corresponding to the asymmetric stretching of methylene (CH2) and methyl (CH3) groups in the PHA monomer units.

The 1700-1750 $cm^{-1}$ spectral region confirms the sample's polyester composition. A prominent absorption band at 1719 $cm^{-1}$ reveals the carbonyl (C=O) stretching vibration of an ester functional group, which is the characteristic of the PHA polymer backbone. The C-O stretching vibration has an additional absorption band at 1283 $cm^{-1}$, whereas the C-O-C stretching vibration has a band at 1184 $cm^{-1}$. The peaks C=O stretch (~1720 $cm^{-1}$), C-O stretch (~1280 $cm^{-1}$), and C-O-C stretch (~1180 $cm^{-1}$) confirm the ester functional group that connects the hydroxyalkanoate monomers in the PHA chain (Kansiz et al., 2000; Mostafa et al., 2020).

In conclusion, the FTIR spectral data support the effective separation of a polyester from Burkholderia sacchari. The combined pattern of absorption bands—from the aliphatic C-H stretches, the prominent ester carbonyl, and the related C-O and C-O-C vibrations—is compatible with the conventional infrared spectrum of Polyhydroxyalkanoates, thus verifying the chemical identity of the collected polymer (Bhatia et al., 2019; Mostafa et al., 2020).

### 3.6. Experimental Results on PHA Production

A Box–Behnken design (BBD) was employed to optimize the fermentation medium for achieving high yields of Polyhydroxyalkanoates (PHA). This statistical approach examined three parameters: incubation temperature (A), pH (B), and incubation time (C), with a total of 17 experimental runs conducted to analyze their effects on PHA yield.

The results indicated that Trials 1 and 17 corresponded to the lowest and highest PHA yields of 3.15 g L-1 and 7.42 g L-1, respectively, which were attained through varying temperature (33 °C and 35 °C), maintaining pH at 7, and adjusting the fermentation time (24 and 48 hours). The study highlights that PHA accumulation in bacterial cells is primarily facilitated by limiting essential nutrients while providing an excess of carbon sources, as noted by Doi et al., (1990).

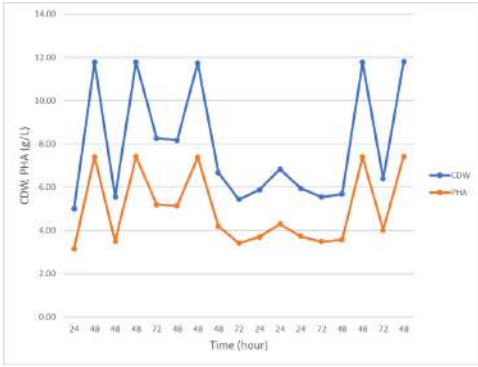


*Figure 3.5: Burkholderia sacchari Growth and PHA Production*

In a study of Burkholderia sacchari, growth and polyhydroxyalkanoate (PHA) production were examined under varying temperatures, pH levels, and incubation periods. The results, illustrated in Figure 4.6, indicate that cell growth persisted until nitrogen depletion in the medium occurred, with PHA accumulation beginning at a cell dry weight (CDW) of approximately 5 g L-1 and peaking at around 12 g L-1. The optimized medium facilitated the highest PHA production, reaching a maximum of 7.42 g L-1 at 48 hours, with a maximum PHA accumulation of 59% from CDW and a minimum yield of 3.15 g L-1. Enhanced cell growth positively correlated with increased PHA production.

### 3.7. Interaction Effects on PHA yield

#### 3.7.1. Interaction Effect Between Temperature and pH

When the temperature is increased from 34 to 37 oC and the pH is increased from 6.5 to 7.5, the yield of PHA varies from 3.15 to 7.42 gL-1. Figure 3.6 shows that when pH increasing from 6.5 to 7 and temperature from 33 to 35 oc maximum yield of 7.42 gL-1 of PHA is obtained and PHA yield is starts to decrease after pH 7 and temperature of to 35 oc. However, productivity couldn't exceed more than 7.42 gL-1 as high temperature slows down the metabolic activity (enzyme activity) of bacteria, reducing their ability to produce PHA (Getachew & Woldesenbet, 2016) and at high and low pH because of its effect on the bioavailability of trace elements and the regulatory enzymes responsible for PHA synthesis (Ranganathan et al., 2022). Temperature is a critical factor in bioprocesses. Temperature changes can cause a variety of microbiological reactions. pH may have effect on the bioavailability of trace elements and the regulatory enzymes responsible for PHA synthesis, ketothiolase, acetoacetyl-CoA reductase, and PHA polymerase, pH had a strong influence on PHA accumulation (Ranganathan et al., 2022). As a result, the yield was influenced by both pH and temperature at the same time. This finding is comparable to that of de Andrade et al, who produced PHA from Burkholderia sacchari using Cheese whey as a carbon source and co substrate and obtained a higher product at a temperature of 35oC and a pH of neutral (de Andrade et al., 2019) B. sacchari grown with glucose at 35 °C demonstrated increased productivity and polymer output.

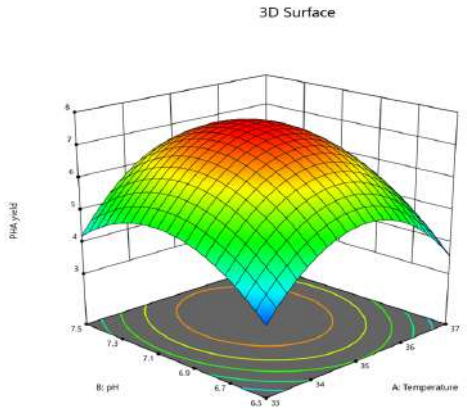


*Figure 3.6: 3D plot of Interaction Effect Between Temperature and pH on the Yield of PHA*

#### 3.7.2. Interaction Effect Between Temperature and Fermentation Time

The interactions of temperature and fermentation period had little effect on PHA yield. This conclusion is derived from both quantitative analysis of variance (ANOVA) and visual representation of the response surface model. They both rise at the same time, with minimal interaction. The P-value for the interaction effect of incubation temperature with time in the ANOVA table is 0.5670,

indicating that there is no significant interaction between these two independent variables on PHA yield. This suggests that adjusting the fermentation temperature has a consistent and independent effect on the final PHA concentration throughout the various fermentation time levels studied, and vice versa. The result depicts a circular contour map of the interaction impact of temperature and pH, indicating that the interaction between variables is not significant (Muralidhar et al., 2001).

### 3.7.3. Interaction Effect Between pH and Fermentation Time

From the ANOVA Table, the p-value of pH and fermentation time was <0.0001, indicates both pH and fermentation time have a greater impact on PHA yield. The observed yield decrease at severe pH levels and temperatures above 35°C is entirely consistent with accepted microbiological principles. Numerous investigations on PHA-producing bacteria demonstrate that optimal polymer production is closely linked to optimal growth conditions. Stresses such as non-optimal pH or supra-optimal temperature cause cellular stress responses, impede important metabolic pathways, and can result in cell lysis, all of which are harmful to high PHA formation (Suryawanshi et al., 2020). As a result, the discovered optimum at pH 7.05-7.1 and 48-50 hours is more than just a statistical result; it also reflects the microbial catalyst's fundamental biological requirements (Tesfaye et al., 2018).

4. Conclusion

It may be concluded that B. sacchari grew better in cultivations using hydrolysates of Napier grass as the sole carbon source at 35 °C, and neutral pH than in other examined scenarios as the strain can consume both hexose and pentose sugars that can be extracted from lignocellulosic materials. In this study, alkaline hydrolysis of Napier grass was done first, followed by enzymatic hydrolysis and glucose rich hydrolysates were obtained. After evaluating the recovered hydrolysates, PHA, biocompatible bioplastic, was synthesized by fermentation and employing the Burkholderia Sacchari strain. This modeling yielded a second-order polynomial equation, indicating an optimal production temperature of 35.38 °C, a pH of 7.05, and a fermentation time of 48.18 hours. The statistical model has a high coefficient of determination ($R^2$) and substantial F-value, indicating its robustness. The improved settings resulted in roughly 7.43 g $L^{-1}$ of PHA, validating the model's accuracy. The results show that B. sacchari is efficient at metabolizing mixed carbohydrates (such as glucose and xylose) from the hydrolysate, hence boosting PHA production and accumulation. This study emphasizes the possibility of combining agricultural waste usage with modern microbial processing and statistical methodologies to provide a sustainable pathway for bioplastic manufacture. To advance the potential of polyhydroxyalkanoate (PHA) as a viable bioplastic, further investigations can be performed on optimizing Napier grass hydrolysates (via NaOH and cellulase), exploring recombinant strains and efficient fermentations with low-cost substrates, and conducting preliminary design and economic feasibility studies to establish scalable PHA manufacturing.

## REFERENCES


1. Acosta-Cárdenas, A., Alcaraz-Zapata, W., & Cardona-Betancur, M. (2018). Sugarcane molasses and vinasse as a substrate for polyhydroxyalkanoates (PHA) production TT - Melazas y vinaza de la caña de azúcar como sustrato para la producción de polihidroxialcanoatos (PHA). Dyna, 85(206), 220–225.
2. Atifah, N., Syamsu, K., & Suryani, A. (2001). POLI- The Fermentation Study on Polyhydroxyalkanoates Produced P roduced by Ralstonia eutropha from Hydrolized Sago Starch as The Carbon Ca rbon Source S ource. 160–171.
3. Basso, V., Machado, J. C., da Silva Lédo, F. J., da Costa Carneiro, J., Fontana, R. C., Dillon, A. J. P., & Camassola, M. (2014). Different elephant grass (Pennisetum purpureum) accessions as substrates for enzyme production for the hydrolysis of

lignocellulosic materials. Biomass and Bioenergy, 71, 155–161.
4. Benedict, S. R. (1909). A reagent for the detection of reducing sugars. Journal of Biological Chemistry, 5(5), 485-487.
5. Bhagowati, P., Pradhan, S., Dash, H. R., & Das, S. (2015). Production, optimization and characterization of polyhydroxybutyrate, a biodegradable plastic by Bacillus spp. Bioscience, biotechnology, and biochemistry, 79(9), 1454-1463.
6. Bhatia, S. K., Gurav, R., Choi, T. R., Jung, H. R., Yang, S. Y., Moon, Y. M., Song, H. S., Jeon, J. M., Choi, K. Y., & Yang, Y. H. (2019). Bioconversion of plant biomass hydrolysate into bioplastic (polyhydroxyalkanoates) using Ralstonia eutropha 5119. Bioresource Technology, 271, 306–315.
7. Choi, Jong Il, & Lee, S. Y. (1997). Process analysis and economic evaluation for poly(3-hydroxybutyrate) production by fermentation. Bioprocess Engineering, 17(6), 335–342.
8. Choi, Jong-il, & Lee, S. Y. (1999). Efficient and Economical Recovery of Poly ( 3-Hydroxybutyrate ) from Recombinant Escherichia coli by Simple.
9. Colombo, B., Pereira, J., Martins, M., Torres-Acosta, M. A., Dias, A. C. R. V., Lemos, P. C., Ventura, S. P. M., Eisele, G., Alekseeva, A., Adani, F., & Serafim, L. S. (2020). Recovering PHA from mixed microbial biomass: Using non-ionic surfactants as a pretreatment step. Separation and Purification Technology, 253(April).
10. De Donno Novelli, L., Moreno Sayavedra, S., & Rene, E. R. (2021). Polyhydroxyalkanoate (PHA) production via resource recovery from industrial waste streams: A review of techniques and perspectives. Bioresource Technology, 331(March), 124985.
11. de Sousa Dias, M. M., Koller, M., Puppi, D., Morelli, A., Chiellini, F., & Braunegg, G. (2017). Fed-batch synthesis of poly(3-hydroxybutyrate) and poly(3-hydroxybutyrate-co-4-hydroxybutyrate) from sucrose and 4-hydroxybutyrate precursors by burkholderia sacchari strain DSM 17165. Bioengineering, 4(2).
12. Doi, Y., Kanesawa, Y., Kunioka, M., & Saito, T. (1990). Biodegradation of microbial copolyesters: poly (3-hydroxybutyrate-co-3-hydroxyvalerate) and poly (3-hydroxybutyrate-co-4-hydroxybutyrate). Macromolecules, 23(1), 26-31.
13. George, A., Sanjay, M. R., Srisuk, R., Parameswaranpillai, J., & Siengchin, S. (2020). A comprehensive review on chemical properties and applications of biopolymers and their composites. International Journal of Biological Macromolecules, 154, 329–338.
14. Getachew, A., & Woldesenbet, F. (2016). Production of biodegradable plastic by polyhydroxybutyrate (PHB) accumulating bacteria using low cost agricultural waste material. BMC Research Notes, 9(1), 1–9.
15. He, C. R., Kuo, Y. Y., & Li, S. Y. (2017). Lignocellulosic butanol production from Napier grass using semi-simultaneous saccharification fermentation. Bioresource Technology, 231, 101–108.
16. Ienczak, J. L., Schmidell, W., & De Aragão, G. M. F. (2013). High-cell-density culture strategies for polyhydroxyalkanoate production: A review. Journal of Industrial Microbiology and Biotechnology, 40(3–4), 275–286.
17. Kansiz, M., Billman-Jacobe, H., & McNaughton, D. (2000). Quantitative determination of the biodegradable polymer poly (β-hydroxybutyrate) in a recombinant Escherichia coli strain by use of mid-infrared spectroscopy and multivariative statistics. Applied and environmental microbiology, 66(8), 3415-3420.
18. K. L. BURDON, T. C. S. A. C. E. K. (1941). rapidly. droplets blue-black.
19. Koller, M. (2018). Chemical and biochemical engineering approaches in manufacturing polyhydroxyalkanoate (PHA) biopolyesters of tailored structure with focus on the diversity of building blocks. Chemical and Biochemical Engineering Quarterly, 32(4), 413-438.
20. Kongkeitkajorn, M. B., Sae-Kuay, C., & Reungsang, A. (2020). Evaluation of napier grass for bioethanol production

through a fermentation process. Processes, 8(5).
21. Kunasundari, B., & Sudesh, K. (2011). Isolation and recovery of microbial polyhydroxyalkanoates. Express Polymer Letters, 5(7), 620–634. https://doi.org/10.3144/expresspolymlett.2011.60
22. Laycock, B., Halley, P., Pratt, S., Werker, A., & Lant, P. (2014). The chemomechanical properties of microbial polyhydroxyalkanoates. Progress in Polymer Science, 39(2), 397–442.
23. López-Rubio, A., Almenar, E., Hernandez-Muñoz, P., Lagarón, J. M., Catalá, R., & Gavara, R. (2004). Overview of active polymer-based packaging technologies for food applications. Food Reviews International, 20(4), 357–387.
24. Lu, X., Li, C., Zhang, S., Wang, X., Zhang, W., Wang, S., & Xia, T. (2019). Enzymatic sugar production from elephant grass and reed straw through pretreatments and hydrolysis with addition of thioredoxin-His-S. Biotechnology for Biofuels, 12(1), 1–11.
25. Marsden, W. L., Gray, P. P., Nippard, G. J., & Quinlan, M. R. (1982). Evaluation of the DNS Method for Analysing Lignocellulosic Hydrolysates. 1016–1022.
26. Marsh, K., & Bugusu, B. (2007). Food packaging - Roles, materials, and environmental issues: Scientific status summary. Journal of Food Science, 72(3).
27. Miller, G. L. (1959). Use of Dinitrosalicylic Acid Reagent for Determination of Reducing Sugar. Analytical Chemistry, 31(3), 426–428.
28. Mostafa, Y. S., Alrumman, S. A., Otaif, K. A., Alamri, S. A., Mostafa, M. S., & Sahlabji, T. (2020). Production and characterization of bioplastic by polyhydroxybutyrate accumulating Erythrobacter aquimaris isolated from
29. mangrove rhizosphere. Molecules, 25(1). Muhammadi, Shabina, Afzal, M., & Hameed, S. (2015). Bacterial polyhydroxyalkanoates-eco-friendly next generation plastic: Production, biocompatibility, biodegradation, physical properties and applications. Green Chemistry Letters and Reviews, 8(3–4), 56–77.
30. Nascimento, V. M., Silva, L. F., Gomez, J. G. C., & Fonseca, G. G. (2016). Growth of Burkholderia sacchari LFM 101 cultivated in glucose, sucrose and glycerol at different temperatures. Scientia Agricola, 73(5), 429-433.
31. Ohimain, E. (2014). Bioenergy Potentials of Elephant Grass, Pennisetum purpureum Schumach. Annual Research & Review in Biology, 4(13), 2215–2227.
32. Oliveira-Filho, E. R., Silva, J. G. P., de Macedo, M. A., Taciro, M. K., Gomez, J. G. C., & Silva, L. F. (2020). Investigating Nutrient Limitation Role on Improvement of Growth and Poly(3-Hydroxybutyrate) Accumulation by Burkholderia sacchari LMG 19450 From Xylose as the Sole Carbon Source. Frontiers in Bioengineering and Biotechnology, 7(January), 1–11.
33. Penkhrue, W., Jendrossek, D., Khanongnuch, C., Pathomareeid, W., Aizawa, T., Behrens, R. L., & Lumyongid, S. (2020). Response surface method for polyhydroxybutyrate (PHB) bioplastic accumulation in Bacillus drentensis BP17 using pineapple peel. PLoS ONE, 15(3), 1–21.
34. Pensri, B., Aggarangsi, P., Chaiyaso, T., & Chandet, N. (2016). Potential of Fermentable Sugar Production from Napier cv. Pakchong 1 Grass Residue as a Substrate to Produce Bioethanol. Energy Procedia, 89, 428–436.
35. Phitsuwan, P., Sakka, K., & Ratanakhanokchai, K. (2016). Structural changes and enzymatic response of Napier grass (Pennisetum purpureum) stem induced by alkaline pretreatment. Bioresource Technology, 218, 247–256.
36. Pradhan, S., Borah, A. J., Poddar, M. K., Dikshit, P. K., Rohidas, L., & Moholkar, V. S. (2017). Microbial production, ultrasound-assisted extraction and characterization of biopolymer polyhydroxybutyrate (PHB) from terrestrial (P. hysterophorus) and aquatic (E. crassipes) invasive weeds. Bioresource Technology, 242, 304–310.

37. Ranganathan, S., Dutta, S., Moses, J. A., & Anandharamakrishnan, C. (2020). Utilization of food waste streams for the production of biopolymers. Heliyon, 6(9).
38. Rehakova, V., Pernicova, I., Kourilova, X., Sedlacek, P., Musilova, J., Sedlar, K., ... & Obruca, S. (2023). Biosynthesis of versatile PHA copolymers by thermophilic members of the genus Aneurinibacillus. International Journal of Biological Macromolecules, 225, 1588-1598.
39. Rodriguez, C., Alaswad, A., Benyounis, K. Y., & Olabi, A. G. (2017). Pretreatment techniques used in biogas production from grass. Renewable and Sustainable Energy Reviews, 68, 1193–1204.
40. Saratale, G. D., Saratale, R. G., Varjani, S., Cho, S. K., Ghodake, G. S., Kadam, A., Mulla, S. I., Bharagava, R. N., Kim, D. S., & Shin, H. S. (2020). Development of ultrasound aided chemical pretreatment methods to enrich saccharification of wheat waste biomass for polyhydroxybutyrate production and its characterization. Industrial Crops and Products, 150(March), 112425.
41. Sayyed, R. Z., Shaikh, S. S., Wani, S. J., Rehman, M. T., Al Ajmi, M. F., Haque, S., & Enshasy, H. A. El. (2021). production of biodegradable polymer from agro-wastes in alcaligenes sp. And pseudomonas sp. Molecules, 26(9), 1–16.
42. Singh, S., Sithole, B., Lekha, P., Permaul, K., & Govinden, R. (2021). Optimization of cultivation medium and cyclic fed-batch fermentation strategy for enhanced polyhydroxyalkanoate production by Bacillus thuringiensis using a glucose-rich hydrolyzate. Bioresources and Bioprocessing, 8(1).
43. Skoog, D. A., Holler, F. J., & Crouch, S. R. (1998). Principles of instrumental analysis (Vol. 203). Philadelphia: Saunders college publishing.
44. Suryawanshi, S. S., Sarje, S. S., Loni, P. C., Bhujbal, S., & Kamble, P. P. (2020). Bioconversion of sugarcane molasses into bioplastic (polyhydroxybutyrate) using Bacillus cereus 2156 under statistically optimized culture conditions. Analytical Chemistry Letters, 10(1), 80-92.
45. Venkata Mohan, S., Nikhil, G. N., Chiranjeevi, P., Nagendranatha Reddy, C., Rohit, M. V., Kumar, A. N., & Sarkar, O. (2016). Waste biorefinery models towards sustainable circular bioeconomy: Critical review and future perspectives. Bioresource Technology, 215, 2–12.
46. Yasuda, M., Ishii, Y., & Ohta, K. (2014). Napier grass (Pennisetum purpureum Schumach) as raw material for bioethanol production: Pretreatment, saccharification, and fermentation. Biotechnology and Bioprocess Engineering, 19(6), 943–950.

# Bio-butanol Production from Hydrolysates of Napier Grass Using Clostridium acetobutylicum: A Comparison of Separate and Semi-Simultaneous Fermentation Processes

**Biruk Yohannes[1] and Dr. Solomon Kiros[1]**

[1]School of Chemical and Bio Engineering, Collage of Technology and Built Environment, Addis Ababa University, P.O. Box 385, Addis Ababa, Ethiopia Corresponding Author:

Biruk Yohannes(E-mail: biruk.yohannes@aau.edu.et)
Dr. Solomon Kiros(E-mail: solomun.kiros@aau.edu.et)

**Abstract**

The quest for sustainable and economically viable biofuels has intensified the focus on lignocellulosic biomass as a renewable feedstock. This study aimed to investigate the valorization of Ethiopian Napier grass (Pennisetum purpureum) for biobutanol production via Acetone-Butanol-Ethanol (ABE) fermentation. The biomass was characterized, subjected to optimized alkaline pretreatment (2.5 wt% NaOH, 1.5 wt% urea, 121°C, 40 min), and enzymatically hydrolyzed. Fermentation using Clostridium acetobutylicum was optimized via Response Surface Methodology (RSM) with a Box-Behnken Design (BBD), and two bioprocessing strategies Separate Hydrolysis and Fermentation (SHF) and Semi-Simultaneous Saccharification and Fermentation (sSSF)—were compared. Compositional analysis revealed that Napier grass contains 35.2% cellulose, 16.9% hemicellulose, and 22.4% lignin, offering 52.1% total fermentable carbohydrates. Alkaline pretreatment effectively delignified the biomass, yielding 28.74 g/L of glucose upon enzymatic hydrolysis. The optimized SHF process (37.5°C, pH 6.0, 64.7 h, 6.5% w/w substrate) produced 15.65 g/L butanol with 0.077 g $L^{-1}$ $h^{-1}$ productivity and 29.5% efficiency. Notably, the sSSF strategy achieved superior results: 17.6 g/L butanol, 0.083 g $L^{-1}$ $h^{-1}$ productivity, and 33.6% efficiency. The distilled biobutanol exhibited favorable fuel properties, including a Higher Heating Value (HHV) of 33,050 kJ/L. This study conclusively demonstrates that Ethiopian Napier grass is a promising feedstock for second-generation biobutanol, with the sSSF strategy offering a more efficient and integrated bioprocessing approach.

**Keywords:** Biobutanol; ABE Fermentation; Napier Grass; Alkaline Pretreatment; Semi-Simultaneous Saccharification and Fermentation (sSSF); Clostridium acetobutylicum.

## 1. Introduction

The 21st century is defined by a dual crisis: the relentless depletion of finite fossil fuel reserves and the escalating environmental catastrophe driven by greenhouse gas (GHG) emissions from their combustion (1). The global energy sector remains predominantly dependent on petroleum, coal, and natural gas, creating profound economic volatility and geopolitical tension (2). More critically, the combustion of fossil fuels is the primary contributor to global warming, leading to a higher frequency of extreme weather events and biodiversity loss (3). This pressing context has triggered an urgent, global quest for sustainable, renewable, and environmentally benign alternatives. Among the various options, biofuels derived from biomass have emerged as a particularly promising pathway for decarbonizing the transportation sector, a major source of $CO_2$ emissions (4). Unlike other renewables, biofuels offer the unique advantage of being storable and compatible with existing internal combustion engine infrastructure and liquid fuel distribution networks, enabling a more

seamless transition.

First-generation biofuels, primarily bioethanol and biodiesel produced from food crops like corn and sugarcane, initially offered hope. However, the "food-versus-fuel" debate, along with concerns over land-use changes and limited GHG reduction potential, severely undermined their sustainability (5). This led to a strategic pivot towards second-generation, or advanced, biofuels produced from non-edible lignocellulosic biomass, which avoids competition with the food supply and utilizes waste materials (6). Among the various biofuel candidates, biobutanol ($C_4H_9OH$), produced via the Acetone-Butanol-Ethanol (ABE) fermentation process has regained significant attention as a next-generation biofuel with properties far superior to the more established bioethanol (7). The ABE fermentation, one of the oldest known industrial bioprocesses, utilizes solventogenic clostridia bacteria, such as Clostridium acetobutylicum, to convert sugars into a solvent mix (8). Butanol, as the primary product, possesses several compelling advantages. Butanol has an energy content of approximately 29.2 MJ/L, which is close to gasoline (32.5 MJ/L) and about 30% higher than ethanol (21.2 MJ/L). This translates directly to better fuel economy (9). In addition, butanol is less prone to absorbing water, which prevents phase separation in gasoline blends and allows it to be blended at higher ratios without requiring vehicle modifications (7). Moreover, due to its lower corrosivity, butanol can be distributed through existing petroleum pipelines, unlike ethanol, significantly reducing distribution costs (8).

Despite these advantages, the commercial viability of ABE fermentation has been historically challenged by high substrate costs and low final product titers, which make recovery and purification energy-intensive (8). The key to overcoming these economic hurdles lies in utilizing inexpensive, abundant feedstocks and optimizing efficient bioprocessing strategies. Lignocellulosic biomass represents the most abundant renewable organic resource on Earth. It is primarily composed of three structural polymers: cellulose, hemicellulose, and lignin, which form a recalcitrant structure that is resistant to microbial and enzymatic deconstruction (10). To access the valuable sugar polymers, a pretreatment step is essential. Alkaline pretreatment has proven particularly effective for herbaceous biomass like grasses, as it efficiently removes lignin with minimal production of fermentation inhibitors like furfural that are common in acid-based pretreatments (11). For a biofuel process to be sustainable and economically viable at a regional level, it must leverage locally abundant and low-cost feedstocks. Napier grass (Pennisetum purpureum Schumach), also known as elephant grass, is a tall, perennial tropical grass native to Sub-Saharan Africa. It is characterized by high biomass yield, rapid growth, strong adaptability to marginal lands, and environmental benefits such as soil erosion prevention (12). Compositionally, Napier grass typically contains 35-45% cellulose, 20-30% hemicellulose, and 15-25% lignin, making it a rich source of fermentable sugars (13).

The conventional process for converting lignocellulosic biomass to biofuels is Separate Hydrolysis and Fermentation (SHF), where the enzymatic hydrolysis and the fermentation are performed in two distinct, sequential steps. While SHF allows each step to be performed at its optimal conditions, it suffers from end-product inhibition of cellulase enzymes by sugars, which can slow down the hydrolysis rate (13). To address this limitation, integrated processes such as Semi-Simultaneous Saccharification and Fermentation (sSSF) have been developed. In sSSF, a dedicated enzymatic hydrolysis step is initiated first, but before completion, the fermenting microorganism is inoculated into the same bioreactor. This allows the initial hydrolysis to proceed at a higher temperature, after which the fermentation begins, and the microorganisms immediately consume the released sugars, alleviating end-product inhibition and potentially leading to higher overall solvent productivity (14)

To address Ethiopia's reliance on fossil fuel imports, this research explores the untapped potential of local Napier grass for producing biobutanol, a superior biofuel. The study aims to determine the feasibility of its conversion using Clostridium acetobutylicum and to establish whether a simultaneous saccharification and fermentation (sSSF) process offers a significant advantage over the conventional separate hydrolysis and fermentation (SHF) method.

## 2. Materials and Methods

Most of the experimental work was done in the laboratories of Addis Ababa institute of Technology at School of Chemical and Bioengineering and School of Civil and Environmental Engineering waste water laboratory. For the production and characterization of bio butanol the following equipment's and chemical were utilized.

*Table 2.1: List of Equipment's and Chemicals*

| No | Equipment's | Model | Chemicals |
|---|---|---|---|
| 1 | Polyethene bag | | Distilled Water |
| 2 | Cooler | | Acetone |
| 3 | Digital Weighing Balance | OHAUS Explorer Pro | Sulfuric acid |
| 4 | pH meter, | Denver Instrument Model 250 | Sodium hydroxide |
| 8 | Water bath | Grant TXF200 | Yeast extract |
| 9 | Incubator, oven, autoclave | | Potassium hydrogen phosphate |
| 10 | Desiccators | | Ammonium chloride |
| 11 | Laminar flow | | Potato Dextrose Agar |
| 13 | Spectrophotometer | Lambda 950 PerkinElmer UV-Vis spectrometer | |
| 14 | Fourier Transform Infrared Spectrometer | Thermo Fisher Nicolet iS5OR | |
| 15 | High Performance Liquid Chromatogram (HPLC) | Waters 600 | |
| 16 | Centrifuge | Universal 320R | |
| 17 | Bomb Calorimeter | Cussons | |

### 2.1. Feedstock Collection and Preparation

Napier grass (Pennisetum purpureum Schumach) was manually harvested from the Menagesha Mushroom Farm, Oromia Special Zone, Ethiopia. The biomass was washed with tap and deionized water, then sun-dried for five days to approximately 10-12% moisture content. The dried biomass was chopped and pulverized using a laboratory-scale cutting mill (Retsch SM 200). The milled biomass was sieved to obtain a uniform particle size of less than 0.84 mm to maximize the surface area for subsequent processing. The powder was further dried in a hot-air oven at 60°C for 24 hours to achieve a constant weight and stored in sealed zip-lock bags at room temperature.

*Figure 1: Napier Grass from Menagesha Mushroom Farm*

### 2.2. Chemical Reagents and Microorganisms

All chemicals used were of analytical grade from Sigma-Aldrich, including NaOH, urea, $H_2SO_4$, and citric acid. The commercial cellulase enzyme complex, Novozymes Cellic® $CTec_2$, was a donated sample. The solventogenic strain Clostridium acetobutylicum was obtained from a commercial culture collection as lyophilized spores. Culture medium components (yeast extract, peptone, minerals) were of microbiological grade from Himedia Laboratories.

### 2.3. Compositional Analysis of Raw Biomass

The proximate and structural composition was determined using standard methods. Moisture content was determined by drying at 105±3°C for 24 hours to constant weight (15; 16). Ash content was measured by incineration in a muffle furnace at 525±25°C for 4 hours (17). The chemical composition was determined using a sequential gravimetric method (18). Extractives were removed via Soxhlet extraction with acetone for 8 hours. Hemicellulose was solubilized by boiling in 0.5M NaOH for 3.5 hours. Acid-insoluble lignin (Klason lignin) was determined by a two-stage acid hydrolysis (72% $H_2SO_4$ followed by dilution and autoclaving). Cellulose content was calculated by difference.

## 2.4. Pretreatment and Enzymatic Hydrolysis

The pretreatment of the biomass was conducted using an alkaline-urea solution comprising 2.5% (w/v) NaOH and 1.5% (w/v) urea at a solid loading of 8% (w/v). The mixture was homogenized and subsequently subjected to autoclaving at 121°C. Following this, the slurry was centrifuged, and the resulting solid residue was neutralized via repeated washing with deionized water and then dried. The enzymatic saccharification of the pretreated substrate was performed at 5% (w/v) solids in a 0.05 M citrate buffer (pH 5.0), employing Novozymes Cellic® CTec2 at a loading of 2 mL per 5 grams of biomass, with 0.02% (w/v) sodium azide added to prevent microbial contamination. The hydrolysis was carried out in a controlled environment at 50°C and 50 rpm for 40 minutes, after which the reaction was quenched by boiling. The resulting hydrolysate was centrifuged, and the supernatant was collected and stored at -20°C for subsequent analytical procedures.

The concentration of total reducing sugars was determined using the DNS method (18). A standard curve was prepared. Absorbance was measured at 540 nm using a UV-Vis spectrophotometer (Lambda 950, PerkinElmer).

## 2.5. Microorganism and Inoculum Preparation

Lyophilized spores of C. acetobutylicum were reactivated under strict anaerobic conditions in Reinforced Clostridial Medium, with a heat shock at 80°C for 10 minutes. For inoculum development, a modified LB-s medium was used [13], containing (per liter): 10 g NaCl, 5 g yeast extract, 0.11 g $FeSO_4 \cdot 7H_2O$, 0.6 g $MgSO_4 \cdot 7H_2O$, and 0.008 g $CaCl_2$ (pH 6.8). Media were pre-reduced by boiling and sparging with nitrogen before autoclaving. The active pre-culture, incubated at 37°C for 18-24 hours, was used as the inoculum.

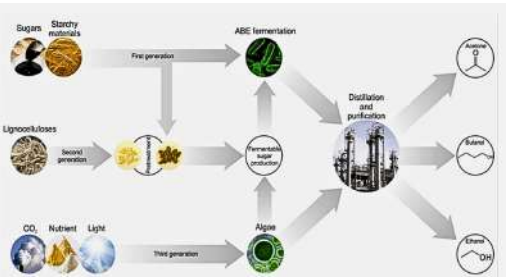


*Figure 2: Schematic Illustration for Solvent Production*

## 2.6. ABE Fermentation Processes

Separate Hydrolysis and Fermentation (SHF): The sugar-rich hydrolysate was used as the carbon source, supplemented with LB-s nutrients. The pH was adjusted to predefined levels (5.0-7.0). Batch fermentations were conducted in 500 mL stirred-tank bioreactors with a 250 mL working volume. Anaerobic conditions were maintained by $CO_2$ sparging. The fermenters were inoculated with 10% (v/v) active pre-culture and run at controlled temperatures (34-40°C) with 150 rpm agitation for 48-96 hours. Semi-Simultaneous Saccharification and Fermentation (sSSF): Alkaline-pretreated biomass (12 g/L) was added directly to the fermentation medium with nutrients and a cellulase enzyme cocktail (3 mL). An initial hydrolysis phase was carried out for 24 hours at 50°C and 200 rpm. Without separation, the temperature was shifted to 37°C, and the pre-culture was inoculated for a 96-hour fermentation phase.

## 2.7. Analytical Methods for Product Characterization

Concentrations of ABE solvents and metabolic acids were quantified using a Waters 600 HPLC system with a UV-Vis detector and a reverse-phase C18 column. The mobile phase was 0.005 M $H_2SO_4$ at a flow rate of 0.5 mL/min (19). Samples were centrifuged and filtered (0.22 µm) before injection. Fourier Transform Infrared (FTIR) Spectroscopy: The chemical identity of distilled biobutanol was confirmed using a PerkinElmer Spectrum 65 FT-IR spectrometer. A thin film was deposited on a NaCl plate, and the spectrum was

recorded from 4000 to 400 $cm^{-1}$.
The Higher Heating Value (HHV) was determined using a Part Cussons bomb calorimeter according to the ASTM D2015 standard method, with benzoic acid calibration (13).

### 2.8. Experimental Design and Statistical Analysis for SHF Optimization

A four-factor, three-level Box-Behnken Design (BBD) was employed using Design-Expert® software (Version 12, Stat-Ease Inc.). The independent variables were: Substrate Concentration (2, 6, 10% w/w), Fermentation Time (48, 72, 96 h), pH (5, 6, 7), and Temperature (34, 37, 40°C). The response variable was Butanol Yield (g/L). The BBD generated 29 randomized runs, including five center points. The data were fitted to a second-order polynomial model. The significance of the model and its terms was evaluated using Analysis of Variance (ANOVA). The model's adequacy was assessed using the coefficient of determination ($R^2$), adjusted $R^2$, and lack-of-fit test.

## 3. Results and Discussion

### 3.1. Characterization of Raw and Pretreated Napier Grass

#### 3.1.1. Proximate and Chemical Composition of Raw Biomass

The initial characterization of the native Napier grass was crucial to evaluate its inherent potential as a fermentation feedstock. The results of the proximate and chemical composition analyses are summarized in Table 2.

*Table 2.2: Compositional Analysis of Native Ethiopian Napier Grass (Dry Basis).*

| Component | Weight Percent |
|---|---|
| Proximate | |
| Moisture | 9.0 ± 0.5 |
| Ash | 7.8 ± 0.3 |
| Chemical | |
| Extractives | 8.7 ± 0.4 |
| Hemicellulose | 16.9 ± 0.6 |
| Acid Insoluble lignin | 22.4 ± 0.7 |
| Cellulose | 35.2 ± 0.8 |
| Total Structural Carbohydrate | 52.1 |

The high total carbohydrate content of 52.1% (comprising 35.2% cellulose and 16.9% hemicellulose) firmly established the suitability of this Ethiopian Napier grass for sugar-platform biorefining. This value is consistent with, and in some cases superior to, other lignocellulosic feedstocks commonly investigated for biofuel production, such as rice straw (~40-50% carbohydrates) and wheat straw (~50-60%) (20). The lignin content of 22.4% is significant and typical for perennial grasses, confirming the necessity of a robust pretreatment step to disrupt the lignocellulosic matrix and expose the polysaccharides for enzymatic attack (10). The ash content of 7.8% was slightly higher than values reported for Napier grass from other regions (e.g., 7.3% (13) ), a variation likely attributable to differences in soil mineral composition and plant age at the time of harvest (20).

#### 3.1.2. Impact of Alkaline-Urea Pretreatment

The alkaline-urea pretreatment resulted in a mass loss of 32.5% in the solid fraction. This substantial reduction is indicative of the effective solubilization and removal of lignin and a portion of the hemicellulose. Visually, the color of the biomass changed from deep green to a light brown, a characteristic sign of delignification. The pretreated solids became more porous and less fibrous, which is a highly desirable outcome for increasing the accessible surface area for cellulase enzymes.
This pretreatment efficacy is critical. Lignin acts as a physical barrier, non-productively binding cellulases and preventing their access to cellulose fibers. By dissolving a large fraction of the lignin, the alkaline pretreatment drastically reduces this recalcitrance. Furthermore, the use of a mild alkali-urea mixture, as opposed to a strong acid, successfully minimized the formation of degradation products like furfural and 5-hydroxymethylfurfural (HMF), which are potent inhibitors of microbial growth during subsequent fermentation (18). This provides a cleaner hydrolysate, reducing the need for costly detoxification steps.

### 3.2. Sugar Yield from Enzymatic Hydrolysis

The effectiveness of the combined pretreatment and enzymatic hydrolysis was quantified by measuring the total reducing sugars (TRS) released into the hydrolysate. The DNS assay, calibrated with a highly linear glucose standard curve ($y = 143.45x + 17$, $R^2 = 0.9822$), was used for this purpose.

The concentration of TRS in the hydrolysate was determined to be 28.74 g/L. Given the 5% (w/v) solid loading during hydrolysis, this translates to a yield of 0.574 g of TRS per gram of pretreated biomass, or a sugar recovery of 3.2 g from the initial 5 g load. This represents a 78% conversion efficiency of the available cellulose in the pretreated biomass into fermentable sugars.

When compared to the study by (7) which recovered 3.9 g of sugar from a similar setup, the yield in this work is approximately 18% lower. This discrepancy can be attributed to several factors inherent to biomass variability, including the specific cultivar of Napier grass, its maturity at harvest, and the distinct climatic and soil conditions in Ethiopia compared to Thailand. Nevertheless, a conversion efficiency of 78% confirms that the pretreatment was successful and that the hydrolytic enzymes were highly effective, providing a rich sugar solution for the subsequent fermentation stage.

### 3.3. Optimization of SHF Process Using Response Surface Methodology

#### 3.3.1. Model Fitting and Statistical Analysis

A Box-Behnken Design (BBD) with 29 experimental runs was executed to investigate the effects of four critical process parameters on butanol yield. The experimental design and the corresponding butanol yields are presented in Table 2. A wide range of butanol production, from 5.6 g/L to 16.8 g/L, was observed, unequivocally demonstrating the profound impact of optimizing the fermentation conditions.

*Table 3.1: Selected Experimental Runs and Butanol Yields from the BBD*

| Run | Substrate (%w/w) | Time (hr) | pH | Temp(oC) | Butanol (g/L) |
|---|---|---|---|---|---|
| 1 | 2 | 48 | 6 | 37 | 5.6 |
| 7 | 10 | 48 | 6 | 37 | 9.8 |
| 13 | 2 | 96 | 6 | 37 | 9.7 |
| 4 | 10 | 96 | 6 | 37 | 10.6 |
| 26 | 6 | 72 | 6 | 37 | 16.3 |
| 29 | 6 | 72 | 6 | 37 | 16.8 |

### 3.4. Analysis of Individual Factor Effects

The optimization of fermentation parameters is crucial for enhancing process efficiency and economic viability. The response surface methodology analysis provided clear insights into the individual and interactive effects of four critical parameters on butanol production. The model predicted maximum butanol production under the following optimized conditions: substrate concentration of 6.51% w/w, fermentation time of 64.65 hours, pH of 6.00, and temperature of 37.46°C. Validation experiments confirmed these predictions, yielding an average butanol concentration of 15.3 g/L, which demonstrated the robustness and accuracy of the optimization model.

#### 3.4.1. Effect of Substrate Concentration

The concentration of fermentable sugars in the hydrolysate significantly influenced butanol production, showing a clear optimum at approximately 6.5% w/w. When substrate concentration increased from 2% to 6% w/w, butanol yield showed a substantial increase from 5.6 g/L to 16.8 g/L. This positive correlation can be attributed to enhanced microbial metabolism and increased solvent production under sufficient nutrient availability. However, further increase in substrate concentration beyond 6.5% w/w resulted in a marked decrease in butanol yield, with the yield dropping to 10.6 g/L at 10% w/w substrate concentration.

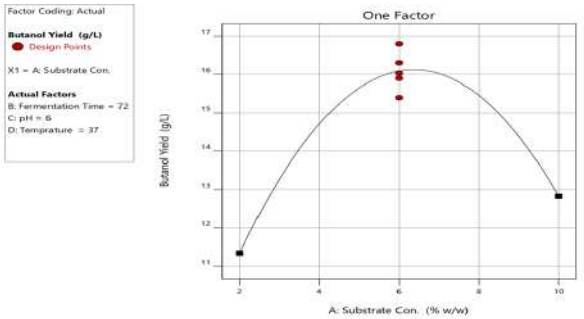


*Figure 3: Effect of Substrate*

This phenomenon represents a classic case of substrate inhibition, where elevated sugar concentrations become toxic to Clostridium acetobutylicum cells. The inhibition mechanism involves osmotic stress and disruption of cellular metabolic pathways, ultimately leading to reduced solvent production. Similar substrate inhibition patterns have been reported in previous studies using lignocellulosic hydrolysates, where optimal sugar concentrations typically range between 5-7% w/w for efficient ABE fermentation. This finding is particularly important for process economics as it defines the maximum substrate loading that can be efficiently utilized without triggering inhibitory effects.

### 3.4.2. Effect of Temperature

Temperature optimization revealed a clear optimum at 37.5°C for butanol production. The butanol yield increased steadily from 7.5 g/L at 34°C to a maximum of 16.8 g/L at 37.5°C, followed by a gradual decline to 10.1 g/L at 40°C. This temperature profile aligns perfectly with the mesophilic nature of Clostridium acetobutylicum, where enzymatic activities and membrane fluidity are optimized within this temperature range.

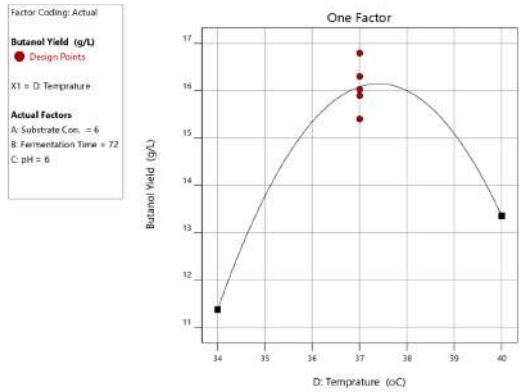


*Figure 4: Effect of Temperature*

The decrease in butanol yield at lower temperatures (34°C) can be attributed to reduced microbial metabolic activity and slower reaction rates of key enzymes involved in the solventogenesis pathway. At elevated temperatures (40°C), the observed decline in productivity likely results from partial denaturation of critical enzymes, disruption of cellular membrane integrity, and increased energy requirements for cellular maintenance. The narrow temperature optimum highlights the sensitivity of solventogenic clostridia to temperature variations and emphasizes the importance of precise temperature control in industrial ABE fermentation processes.

### 3.4.3. Effect of Fermentation Time

The time course of ABE fermentation exhibited characteristic biphasic behavior, with butanol production showing a strong dependence on fermentation duration. Butanol accumulation increased progressively during the first 72 hours of fermentation, reaching maximum concentrations of 16.3-16.8 g/L. Beyond this point, extended fermentation time up to 96 hours resulted in either a plateau or slight decrease in butanol concentration.

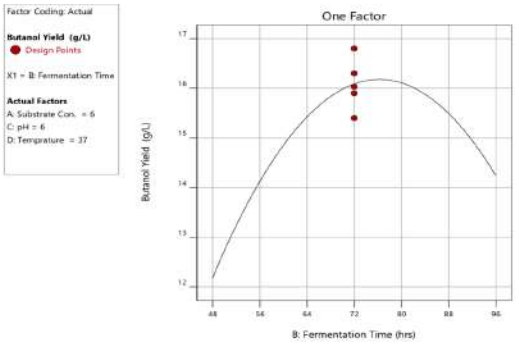


*Figure 5: Effect of Fermentation Time*

The initial increase corresponds to the active solventogenic phase, where the culture shifts from acid production to solvent generation, accompanied by the reassimilation of previously accumulated acetic and butyric acids. The subsequent decline after 72 hours can be attributed to multiple factors: butanol toxicity to the producing microorganisms, nutrient depletion in the fermentation medium, and possible degradation of solvents or conversion to other metabolites. The identification of optimal fermentation time at 64.65 hours represents a balance between maximizing product yield and minimizing process time, which is crucial for enhancing volumetric productivity in industrial applications.

### 3.4.4. Effect of pH

The pH of the fermentation medium exerted a profound influence on the metabolic behavior of Clostridium acetobutylicum, directly affecting the transition from acidogenesis to solventogenesis. Butanol production showed a distinct optimum at pH 6.0, with yields decreasing significantly at both lower (pH 5.0) and higher (pH 7.0) pH values. At pH 5.0, the culture predominantly remained in the acidogenic phase, accumulating acetic and butyric acids with minimal solvent production

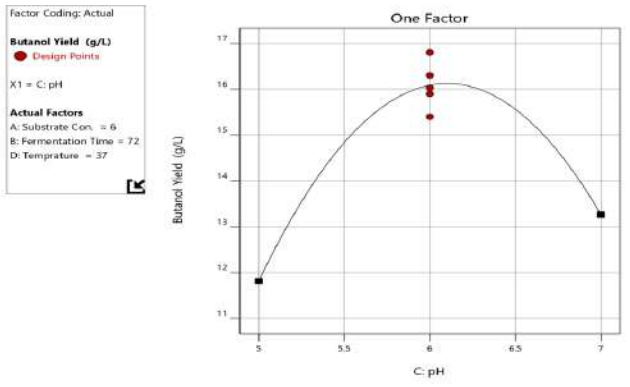


*Figure 6: Effect of pH*

The optimal pH of 6.0 effectively triggered the metabolic shift toward solventogenesis, enhancing the expression of genes encoding solvent-forming enzymes and facilitating the reassimilation of organic acids. The reduced performance at pH 7.0 was primarily attributed to the accumulation of sodium chloride formed during pH adjustment using NaOH, which is a known inhibitor of clostridial growth and solvent production. This finding underscores the critical importance of pH control strategy in ABE fermentation and suggests that alternative buffering systems or neutralizing agents might be beneficial for maintaining optimal pH without introducing inhibitory compounds.

### 3.4.5. Interaction Effect of Sugar Concentration and Fermentation Time

The interaction between substrate concentration and fermentation time revealed complex, non-linear effects on butanol production. At shorter fermentation times (48 hours), systems with higher substrate concentration (10% w/w) produced significantly more butanol (9.8 g/L) compared to systems with lower substrate concentration (2% w/w), which yielded only 5.6 g/L. This relationship, however, changed dramatically with extended fermentation time.

At 96 hours of fermentation, the difference in butanol yield between high (10% w/w) and low (2% w/w) substrate concentrations diminished considerably. The low-substrate system showed substantial improvement, reaching 9.7 g/L, while the high-substrate system showed only marginal improvement to 10.6 g/L. This convergence indicates that given sufficient time, even low substrate concentrations can be efficiently converted, whereas high substrate concentrations, while providing initial productivity advantages, ultimately lead to inhibition that limits complete substrate utilization.

The most favorable combination was observed at intermediate substrate concentration (6% w/w) and fermentation time (72 hours), which yielded the maximum butanol production of 16.8 g/L. This optimal point represents a balance between providing adequate substrate for microbial growth and solvent production while avoiding the inhibitory effects associated with high substrate concentrations. The interaction analysis suggests that fed-batch strategies, where substrate is added gradually rather than all at once, could potentially overcome the inhibition limitations and further improve process performance.

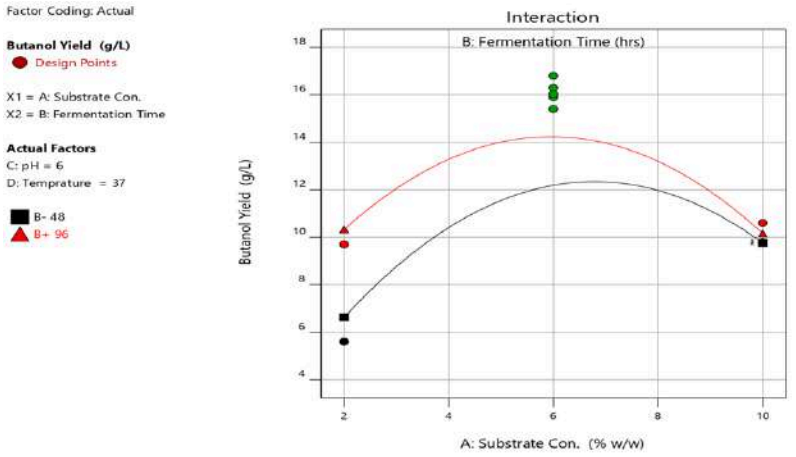


*Figure 7: Interaction Effect of Sugar Concentration and Fermentation Time*

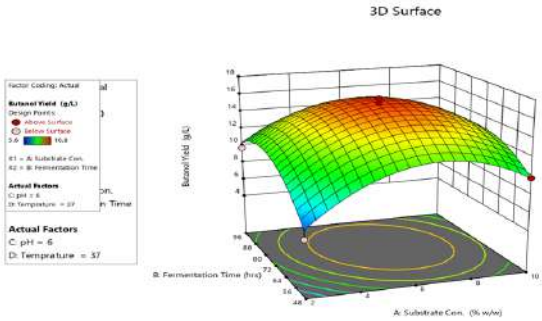


*Figure 8: 3D surface interaction between Sugar concentration and Fermentation time*

### 3.5. Comparative Performance: SHF vs. sSSF

The performance of the optimized SHF process was compared with the Semi-Simultaneous Saccharification and Fermentation (sSSF) process. The results, summarized in Table 3, reveal a clear advantage for the integrated process.

*Table 4.1: Comparison of SHF and sSSF Fermentation Performance.*

| Parameter | SHF Process | sSSF Process |
|---|---|---|
| Final Butanol Titer (g/L) | 15.3 ± 0.3 | 17.6 ± 0.4 |
| Total Fermentation Time (h | 64.7 | 120 (96 h fermentation + 24 h hydrolysis) |
| Butanol Productivity (g/L/h) | 0.077 | 0.083 |
| Process Efficiency (%)* | 29.5 | 33.6 |
| *Efficiency = (Mass of butanol produced / Theoretical mass of butanol from sugar consumed) × 100 | | |

The sSSF process achieved a 15% higher final butanol titer (17.6 g/L vs. 15.3 g/L) and a 7.8% higher productivity compared to the optimized SHF process. The primary reason for this enhancement is the alleviation of end-product inhibition during the enzymatic hydrolysis phase. In SHF, the released sugars (cellobiose and glucose) accumulate and inhibit the cellulase enzymes, slowing down the overall hydrolysis rate. In sSSF, the fermenting cells immediately consume these sugars as they are released, maintaining a low sugar concentration in the broth. This keeps the hydrolysis rate high and results in a greater total amount of sugar being converted to solvents over the course of the process (14).
Furthermore, the sSSF process, while having a longer total process time (120 h vs. 64.7 h), consolidates two-unit operations into a single vessel, which can lead to reductions in capital and operational costs at a larger scale by eliminating the need for a separate hydrolysis reactor and associated transfer steps.

The process efficiencies of 29.5% for SHF and 33.6% for sSSF are within the range reported for other lignocellulosic feedstocks. For instance, (21) reported 36% efficiency from barley straw, (22) achieved 19% from pine wood. The slightly lower than theoretical maximum efficiency (~40%) is expected due to carbon diversion towards cell mass, the production of other solvents (acetone, ethanol), and maintenance energy.

### 3.6. Comparative Performance of SHF and sSSF Processes

The validation experiment at the predicted optimum conditions for SHF (6.5% w/w, 64.7 h, pH 6.0, 37.5°C) yielded an average of 15.3 g/L of butanol, closely matching the model's prediction of 15.65 g/L. This corresponds to a productivity of 0.077 g $L^{-1}$ $h^{-1}$ and a process efficiency of 29.5% (based on the mass of butanol produced per mass of theoretical sugar available).

In contrast, the sSSF process, under similar fermentation conditions, achieved a significantly higher butanol titer of 17.6 g/L. This resulted in a higher productivity of 0.083 g $L^{-1}$ $h^{-1}$ and an improved process efficiency of 33.6%. The superior performance of sSSF can be attributed to the continuous release of glucose during hydrolysis, which immediately becomes available for fermentation.

This reduces the accumulation of sugars that can cause catabolite repression or substrate inhibition and minimizes the feedback inhibition of cellulases by their end-products (cellobiose and glucose), leading to a more efficient and rapid overall conversion.

3.7. Comprehensive Characterization of Biobutanol Product

The successful production of biobutanol was confirmed and quantified through a multi-faceted characterization approach. The analyses not only verified the chemical identity and purity of the product but also critically assessed its key properties as a potential fuel.

### 3.7.1. Fuel Property Assessment: Higher Heating Value (HHV)

The energy content of a biofuel is a paramount property determining its viability as a gasoline substitute. The Higher Heating Value (HHV) of the distilled biobutanol produced in this study was determined to be 33,050 kJ/L (6,757.86 kcal/L) using a bomb calorimeter.

Significance and Comparison: This value is in close agreement with the HHV reported for commercial Petro-butanol, which is approximately 33,170 kJ/L (13), and is substantially higher than that of bioethanol (~23,322 kJ/L). This 30% higher energy density than ethanol is a critical advantage, as it translates directly to a longer driving range for vehicles using butanol-blended or pure butanol fuel. When compared to gasoline (~31,929 kJ/L), the biobutanol's HHV is remarkably similar, confirming its capability to be a "drop-in" fuel that can replace gasoline liter-for-liter without sacrificing engine performance or fuel economy, unlike lower-energy-density alternatives.

Implication for Blending: The high HHV underscores one of the principal benefits of biobutanol over ethanol. While ethanol blending typically reduces the energy content of the fuel mix, leading to a 2-5% decrease in fuel economy for a 10% blend, butanol's comparable energy content minimizes this penalty. This makes the biobutanol derived from Napier grass a technically superior and more economically attractive biofuel for blending mandates and future biofuel adoption.

### 3.7.2. Molecular Fingerprinting: Fourier Transform Infrared (FTIR) Spectroscopy

FTIR analysis was employed to confirm the molecular structure and identify the functional groups present in the purified fermentation product. The resulting spectrum (Figure 7) displayed all the characteristic absorption bands of a primary alcohol, unequivocally confirming the product as butanol.

**Detailed Spectral Analysis:**

O-H Stretch: A broad and intense band centered at ~3320 $cm^{-1}$ is indicative of the O-H stretching vibration. The breadth of this band is characteristic of intermolecular hydrogen bonding, which is typical for liquid alcohols and confirms the presence of the hydroxyl (-OH) group. C-H Stretch: The spectrum showed distinct peaks in the 2950-2850 $cm^{-1}$ region. Specifically, the peaks at ~2950 $cm^{-1}$ and ~2870 $cm^{-1}$ are attributed to the asymmetric and symmetric C-H stretches of methyl ($-CH_3$) groups. The peaks at ~2925 $cm^{-1}$ and ~2855 $cm^{-1}$ correspond to the asymmetric and symmetric C-H stretches of methylene ($-CH_2-$) groups. This pattern is a definitive signature of the four-carbon alkyl chain of butanol.

C-O Stretch: A strong and prominent absorption band at ~1055 $cm^{-1}$ is a definitive marker for the C-O stretching vibration in primary alcohols. This band is crucial for distinguishing butanol from secondary or tertiary alcohols and confirms the structure of 1-butanol.

Conclusion from FTIR: The simultaneous presence of these three key vibrational modes —O-H, C-H (of a C4 chain), and C-O (primary)—provides conclusive evidence that the target product, biobutanol, was successfully synthesized and recovered from the ABE fermentation broth. This analysis rules out significant contamination from other solvents or residual water at a molecular level.

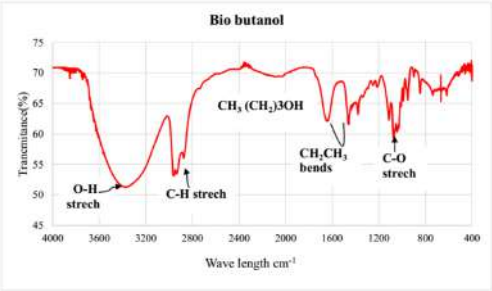


*Figure 8: FTIR spectrum of the purified biobutanol product, showing characteristic O-H, C-H, and C-O stretching vibrations.*

### 3.7.3. Process Monitoring and Quantification: High-Performance Liquid Chromatography (HPLC)

HPLC analysis served a dual purpose: it provided a quantitative profile of all major metabolites in the fermentation broth and confirmed the identity of butanol based on its retention time.

Chromatographic Profile: A representative HPLC chromatogram of the fermentation broth at the end of the optimized batch is presented in Figure 8. The identification of compounds was based on the retention times of authentic standards.

Peak Identification and Quantification:
Residual Glucose (~23 min): A small peak indicated the presence of unconsumed glucose, confirming that the fermentation was not entirely substrate-limited and could potentially be optimized further with a higher microbial load or different feeding strategy.

Acetic Acid (~40 min) and Butyric Acid (~58 min): The presence of these organic acids is a hallmark of the ABE fermentation pathway.

Their concentrations were relatively low at the time of sampling, which is expected during the solventogenic phase, as C. acetobutylicum reassimilates these acids to produce solvents.

ABE Solvents: The chromatogram clearly shows the peaks for the target solvents: Ethanol (~24 min), Acetone (~59 min), and Butanol (~95 min). The butanol peak was the largest among the solvents, which aligns with the typical product ratio for C. acetobutylicum.

Yield and Ratio Calculation: The area under each peak was integrated and converted to concentration using calibration curves. This allowed for the precise calculation of the final butanol titer (17.6 g/L in sSSF), as well as the acetone and ethanol titers. The typical ABE ratio observed was approximately 3:6:1 (Acetone:Butanol:Ethanol), which is consistent with reported literature for this strain. The HPLC data was therefore critical for calculating the precise yield, productivity, and mass balance of the fermentation process.

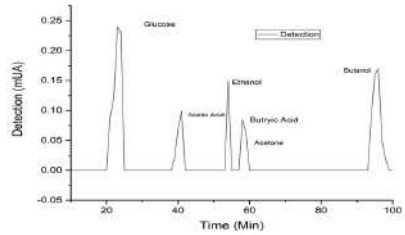


*Figure 10: HPLC chromatogram of the ABE fermentation broth, showing the separation and identification of residual glucose, metabolic acids (acetic, butyric), and solvent products (ethanol, acetone, butanol).*

The collective data from HHV, FTIR, and HPLC provides a robust and conclusive characterization of the biofuel product. HPLC confirmed that the target process produced butanol as the major solvent and provided quantitative data on the entire fermentation profile. FTIR verified the molecular structure of the distilled product as 1-butanol, ensuring its chemical identity. HHV validated that the produced biobutanol possesses the essential fuel property of high energy density, making it a functionally equivalent substitute for fossil-derived fuels. This multi-technique approach leaves no doubt about the success of the bioconversion process and the quality of the final product, firmly establishing the potential of Napier grass as a feedstock for high-quality biobutanol production.

## 4. Conclusion

This study examined the possibility of producing bio-butanol from Napier grass. Napier grass has 52.1 % carbohydrates which makes it a potential biomass for ABE fermentation to produce bio-butanol. 78 % of reducing sugar yield was obtained by alkaline pretreatment jointly with enzymatic hydrolysis that showed the potential of Napier grass to be efficiently transferred from polysaccharides to its monomer structure. In addition, this study showed production of butanol by using C. acetobutylicum bacteria and ABE fermentation. Experimental design was conducted by BBD to study the effect of four operational parameters, pH, temperature, sugar substrate concentration, and fermentation time. The optimum operating condition was found at temperature of 37.459 °C, pH of 6, fermentation time of 64.65 hrs, and 6.51 % w/w of reducing sugar concentration. At these optimum operating conditions, the yield of butanol was 15.649 g L-1

The maximum observed value of butanol productivity recorded was 0.077 g L-1hr-1 and 29.5 % efficiency for separated enzyme hydrolysis and ABE fermentation process while 0.083 g L-1hr-1 productivity and 33.6 % efficiency was obtained by sSSF process.

Based on this study it is evident that the chosen method of optimization was efficient and sSSF process has high productivity and also it minimizes the process. From this it can be conclude that the selected model was adequately fit the data of response variable and Napier grass is excellent potential biomass for production of bio-butanol.

Chemical characterization of bio-butanol was performed and its higher heating value of 6,757.86 kcal L-1 fulfills the desired range to be used as fuel. In addition, FTIR spectroscopy result of the optimized bio butanol product exhibited O-H, C-O, C-H, – CH2, and –CH3 functional groups on the specified wavenumbers and confirms the presence of butanol in the product

This study successfully establishes a complete and optimized pathway for biobutanol production from underutilized Ethiopian Napier grass.

## REFERENCES


1. Energy, Agency. International. World Energy Outlook 2022. Paris : IEA Publications;, 2022.
2. Production of first and second generation biofuels:. Naik SN, Goud VV, Rout PK, Dalai AK. 2, s.l. : Renew Sustain Energy Rev., 2010, Vols. 14:578-97.
3. Fermentative production of butanol—the industrial perspective. Green, E. M. 3, s.l. : Curr Opin Biotechnol., 2011, Vols. 22:337-43.
4. Biobutanol production from renewable resources: Metabolic engineering and process development. Jang YS, Malaviya A, Cho C, Lee J, Lee SY. 10, s.l. : Biotechnol Bioeng, 2012, Vols. 109:2437-59.
5. Bio-butanol as a new generation of clean alternative fuel for SI (spark ignition) and CI (compression ignition) engines. Zhen X, Wang Y, Liu D. s.l. : Renew Energy., 2020, Vols. 147:2494-521.
6. Features of promising technologies for pretreatment of lignocellulosic biomass. Mosier N, Wyman C, Dale B, Elander R, Lee YY, Holtzapple M, et al. 6, s.l. : Bioresour Technol, 2005, Vols. 96:673-86.
7. Effects of the pretreatment method on enzymatic hydrolysis and ethanol fermentability of the cellulosic fraction from elephant grass. Eliana C, Jorge R, Juan P, Luis R. 2014, Vols. 118:41-47.
8. Lignocellulosic butanol production from Napier grass using semi-simultaneous saccharification fermentation. He CR, Kuo YY, Li SY. s.l. : Bioresour Technol. , 2017, Vols. 231:101-8.
9. Modeling semi-simultaneous saccharification and fermentation of ethanol production from cellulose. Shen J, Agblevor FA. 8, s.l. : Biomass Bioenergy., 2010, Vols. 34:1098-107.
10. Determination of Structural Carbohydrates and Lignin in Biomass. Sluiter A, Hames B, Ruiz R, Scarlata C, Sluiter J, Templeton D, et al. s.l. : Golden, CO:National Renewable Energy LaboratoryTechnical

Report, 2008.
11. Coordinated Development of leading biomass pretretment technologies. M, Lee.Y. Wyman.C. Dale.B.Elandar R. Holtzapple M. Landisch. 3, 2005, Vols. 31426-8.
12. Nyambati, E,M. Muyekho. F.N. Onginjo.E. & Lusweti.C.M. Production ,Characterization and Nutrational Quality of NApier Grass. Kenya : s.n., 2010, Vols. 6(3):774-81.
13. Experimental study of the effect of 1-butanol addition on the physicochemical properties of diesel fuel and emissions of a compression ignition engine. Energy Fuels. Kuszewski, H. 11, 2018, Vols. 32:619-31.
14. Impact of pH and butyric acid on butanol production during batch fermentation using a new local isolate of Clostridium acetobutylicum. Al-Shorgani NKN, Kalil MS, Yusoff WMW, Hamid AA. 2, s.l. : Saudi J Biol Sci., 2018, Vols. 25:339-48.
15. Enhanced sugar production from pretreated barley straw by additive xylanase and surfactants in enzymatic hydrolysis for acetone–butanol–ethanol fermentation. . Yang M, Zhang J, Kuittinen S, Vepsäläinen J, Keinänen M, Pappinen A. s.l. : Bioresour Technol., 2015, Vols. 189: 131-7.
16. ASTM D1102-84: Standard Test Method for Ash in Wood. International., ASTM. PA, USA: : West Conshohocken, ASTM International;, 2014.
17. Autohydrolysis: A promising pretreatment for the improvement of acetone, butanol, and ethanol production from woody materials. Amiri H, Karimi K. s.l. : Chem Eng Sci, 2015, Vol. 137 .
18. Use of Dinitrosalicylic Acid Reagent for Determination of Reducing Sugar. Analytical Chemistry. Miller, G L. 3, 1959, Vols. 31:426-428.
19. Acetone-butanol-ethanol fermentation analysis using only high performance liquid chromatography. Analytical Methods. Kumar M, Saini S, Gayen K. 3, 2014, Vols. 6:774-781.
20. Comprehensive characterization of Napier grass as a feedstock for thermochemical conversion. Energies. Mohammed IY, Abakr YA, Kazi FK, Yusup S, Alshareef I,. 5, Shangani : s.n., 2015, Vols. 8 3403-3417.
21. Enhanced sugar production from pretreated barley straw by additive xylanase and surfactants in enzymatic hydrolysis for acetone–butanol–ethanol fermentation. Bioresource Technology. Yang M, Zhang J, Kuittinen S, Vepsäläinen J, Keinänen M, Pappinen A. 2015, Vols. 189:131-137.
22. Autohydrolysis: A promising pretreatment for the improvement of acetone, butanol, and ethanol production from woody materials. Amiri H, Karimi K. s.l. : Chemical Engineering Science, 2015, Vols. 137:722-729.
23. Experimental study of the effect of 1-butanol addition on the physicochemical properties of diesel fuel and emissions of a compression ignition engine. Energy & Fuels. Kuszewski, H. 11, 2018, Vols. 32:619-631.

# Enhancing Energy Security in Ethiopia through Natural Gas and Geothermal Development
## (Review Article)

**Ramadan Ahmed, University of Oklahoma**

**Abstract**

Over the past twenty years, Ethiopia has significantly expanded electricity access through large-scale hydropower and wind energy projects. However, heavy reliance on hydropower, which currently provides nearly 88% of electricity, makes the national power system more vulnerable to climate change, frequent droughts, and unpredictable rainfall. This study examines the strategic importance of diversifying Ethiopia's energy mix by developing natural gas and geothermal resources. The paper reviews the country's natural gas resources and ongoing gas-to-power infrastructure projects, highlighting their role in enhancing grid stability and industrial development. It further evaluates Ethiopia's vast geothermal potential within the East African Rift System, including the status of existing and planned geothermal projects. Emerging geothermal technologies, including Enhanced Geothermal Systems (EGS), Advanced Geothermal Systems (AGS), and SuperHot Rock (SHR) systems, are discussed as transformative pathways for expanding geothermal deployment beyond conventional hydrothermal limits. The current study shows that strategically combining natural gas and geothermal energy can greatly enhance energy security, lower climate-related risks in power generation, and promote sustainable economic growth in drought-prone areas. The results highlight that developing diverse renewable and transitional energy sources is crucial for creating a resilient and reliable power system in Ethiopia.

**Keywords:** Energy diversification, Sustainability, Natural gas, geothermal energy, Hydropower vulnerability, Climate resilience.

### 1. Introduction

Over the past two decades, Ethiopia has made significant progress in expanding electricity generation, positioning itself as one of Africa's leading renewable-energy-driven power systems [1–3]. Access to electricity in rural Ethiopia has increased markedly (Fig. 1) since 2005, driven by the construction of large dams and the development of wind farms. A majority of the country's electricity is generated from clean energy sources. For instance, diesel-based thermal plants account for only about 3.51% of electricity generation, while hydropower accounts for 88.25%. The remaining shares include 7.49% wind power, 0.58% biomass from the Reppie waste-to-energy facility, and 0.17% geothermal power [2,4]. By relying heavily on renewable energy, the country has limited greenhouse gas emissions.

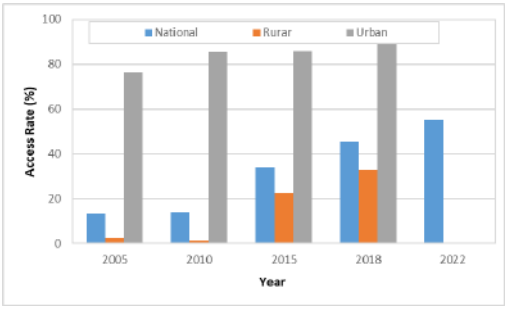


*Fig. 1: Access to electricity in Ethiopia, adopted from previous studies [8,9]*

Although these achievements have been made, hydropower accounts for approximately 88% of the country's energy mix, leaving the power system highly vulnerable to climate change [2,5]. The production of hydroelectricity is inherently affected by hydrological factors, especially the seasonal and inter-annual variability of rainfall. A prolonged drought and irregular precipitation patterns have

increasingly impacted reservoir levels and power generation in recent years [6,7]. While hydropower is a clean, environmentally friendly energy source, its operational performance is strongly influenced by seasonal rainfall fluctuations, which are projected to increase as climate change progresses. In the face of climate change, rainfall variability and extreme weather events are expected to intensify, further increasing the risk to hydropower reliability.

Increasing exposure to climate-induced energy insecurity underscores the urgent need for comprehensive energy diversification in Ethiopia. Heavy reliance on hydropower has made the national electricity system increasingly vulnerable to climate variability, particularly prolonged droughts that lower reservoir levels and constrain power generation. To enhance grid resilience, ensure a reliable electricity supply, and support sustained economic development, Ethiopia must expand its portfolio of alternative and complementary energy sources, including solar, wind, natural gas, and geothermal.

Ethiopia is endowed with vast solar resources, with many regions receiving high year-round solar radiation, offering strong potential for large-scale solar energy deployment and decentralized off-grid systems. In addition, several high-wind corridors across the country are well suited to large-scale wind farms that can significantly contribute to national power generation.

The Ogaden Basin holds substantial natural gas reserves, which, if responsibly developed, could serve as a dispatchable fuel to complement intermittent renewables.

Furthermore, the Ethiopian Rift Valley contains enormous geothermal potential, offering a reliable baseload energy option largely independent of climate variability. These resources are currently underdeveloped. Therefore, strategic development of these diverse energy resources would strengthen grid stability, reduce dependence on hydropower, and support Ethiopia's long-term energy security.

Beyond enhancing grid stability and national energy security, the strategic development of diversified energy resources would substantially reduce pressure on Ethiopia's forest ecosystems. Expanding access to modern energy sources such as electricity, natural gas, and geothermal heat would provide viable alternatives to traditional biomass fuels. This transition would decrease household dependence on firewood and charcoal, mitigating deforestation, land degradation, and associated environmental impacts.

The objective of this paper is to examine the strategic importance of diversifying Ethiopia's energy mix to reduce dependence on weather-sensitive resources. The paper discuss the role of natural gas and geothermal energy in strengthening energy security, improving power system resilience, and supporting sustainable development in drought-prone regions.

## 2. Methodology

This study uses a structured review methodology to evaluate the roles of natural gas and geothermal energy in enhancing Ethiopia's energy security and climate resilience. Peer-reviewed journal articles, technical reports, policy documents, and datasets from international organizations, government agencies, and industry sources were systematically reviewed to assess the status, potential, and challenges of Ethiopia's energy sector. Particular emphasis was placed on literature addressing hydropower vulnerability to climate variability, natural gas resource development, and geothermal energy deployment within the East African Rift System.

Quantitative data on the electricity generation mix, resource reserves, geothermal gradients, and installed capacities were compiled from reliable sources. Spatial and geological information on geothermal prospects was

synthesized from regional studies and geophysical investigations to identify high-potential areas, including the Main Ethiopian Rift and the Afar region.

The analysis integrates emerging geothermal technologies, including EGS, AGS, and superhot geothermal systems, to evaluate their technical feasibility and long-term contribution to energy diversification. Finally, a phased implementation roadmap was developed by synthesizing technical, economic, and policy insights to align short- and long- term energy development pathways with Ethiopia's sustainability and energy security objectives.

## 3. Natural Gas as a Strategic Energy Option

### 3.1 Gas Reserves

Ethiopia has significant onshore natural gas resources, particularly in the Ogaden region, where natural gas was identified through an extensive exploration program that included the drilling of 19 wells. The exploration confirmed the presence of a substantial natural gas volume of approximately 21.3 billion cubic meters. In addition to the Ogaden Basin, Ethiopia's hydrocarbon potential is complemented by oil and gas occurrences in other regions, including Mekele, Metema, South Omo, and Gambella [10]. As of 2017, Ethiopia is estimated to hold approximately 28 billion cubic meters of proven natural gas reserves, representing about 0.013% of global gas reserves [11]. The actual reserve could be higher than reported due to recent discoveries [12]. While modest on a worldwide scale, these reserves constitute a strategically important domestic energy resource with strong potential to support power generation, industrial development, and energy diversification.

### 3.2 Existing Exploration and Development Status

In recent years, progress has been made in developing gas resources in the Ogaden Basin. Ethiopia officially launched the first phase of the Ogaden Liquefied Natural Gas (LNG) Project in Calub on October 2, 2025. The multipurpose facility is designed to produce approximately 111 million liters of gas annually and generate up to 1,000 MW of electricity, marking a major milestone in the country's gas-to-power goals [13]. The second phase of the Ogaden gas project, expected to be completed in the coming years, is anticipated to be much larger, with an annual production capacity of 1.3 billion liters. Once fully developed, the project is expected to significantly enhance Ethiopia's energy security, reduce reliance on hydropower, and support large-scale industrialization.

### 3.3 Infrastructure Development

Ethiopia is expanding its downstream and midstream energy infrastructure to support the development of its natural gas and petroleum resources. As part of a major industrialization effort, the country plans to build its first oil refinery with an annual processing capacity of 3.5 million metric tons (about 70,000 barrels per day). The refinery will process domestically produced crude oil, primarily from the Hilala oil field in the Ogaden Basin. Once operational, it is expected to supply nearly 70% of Ethiopia's current national fuel demand, significantly reducing dependence on imported refined petroleum products and enhancing national energy security [14].

Alongside the refinery plan, Ethiopia is developing gas-processing infrastructure to enable value-added use of its natural gas resources. A major urea fertilizer plant with a projected capacity of 3 million metric tons per year is planned for the same region. The fertilizer plant will be supplied with natural gas from the Calub gas fields via a 108-km dedicated pipeline, establishing a critical link between upstream gas production and downstream industrial consumption [14]. This integrated pipeline–refinery–fertilizer complex is a cornerstone of Ethiopia's gas-to-industry strategy, enabling domestic fuel production, supporting agricultural productivity, and maximizing the economic value of indigenous hydrocarbon resources. To address security challenges associated with midstream

infrastructure in the region, risk-mitigation measures such as phased pipeline construction, enhanced security coordination, route selection, physical asset protection, and public–private partnership frameworks are essential.

Although liquefied natural gas (LNG) export options were planned earlier, the current infrastructure strategy prioritizes domestic natural gas use for power generation, refining, and fertilizer production, thereby reinforcing energy diversification and long-term industrial development.

### 3.4 Regulatory Frameworks

The regulatory framework governing natural gas and liquefied natural gas (LNG) production and transportation is crucial for ensuring safe operations, environmental protection, and energy security. Traditionally, natural gas exploration and production are governed by government policies and state laws that establish licensing procedures, production-sharing mechanisms, and royalty and tax systems. Regulatory authorities issue exploration and production licenses, approve field development plans, and enforce technical, environmental, and safety standards. Environmental impact assessments are essential before drilling and field development to manage emissions, minimize land disturbance, and safeguard groundwater resources [15].

Gas transportation via pipelines and processing plants is governed by strict pipeline safety regulations, design codes, and pressure-control standards [16]. Continuous monitoring, leak-detection systems, and emergency response planning are mandatory for operational safety [17]. LNG facilities are regulated under specialized frameworks that cover liquefaction plants, storage tanks, and LNG carriers [18]. These regulations address cryogenic safety, hazardous-area classification, and boil-off gas (BOG) management. Despite LNG's role in the global energy mix and its status as a cleaner alternative to traditional fossil fuels, managing BOG remains a significant challenge. Uncontrolled BOG can compromise safety, cause resource losses, and contribute to environmental pollution [19]. Although natural gas is the cleanest fossil fuel, it is a greenhouse gas with 22 times the global warming impact of $CO_2$ [20].

## 4. Geothermal Energy Option

### 4.1 Global Geothermal Power Production

Although geothermal energy has been part of global energy systems for more than a century, its contribution has remained limited [21]. Today, advances in technology are unlocking access to previously untapped geothermal resources, expanding their role in energy systems worldwide. Geothermal power is now being installed and utilized in many countries (Fig. 2), including the United States, Indonesia, the Philippines, Turkey, New Zealand, Mexico, Italy, Kenya, Iceland, and Japan, which rank among the world's top ten geothermal energy users [8]. As a component of a sustainable power mix, geothermal energy holds significant promise, and its global electricity supply has increased steadily (Fig. 3) since 2010, in line with environmental and sustainability efforts. However, despite this continued growth, the pace of development remains slow due to major technological challenges, including drilling deep wells into high-temperature, high-pressure reservoirs, maintaining long-term reservoir productivity, and environmentally responsible disposal of minerals and gases dissolved in geothermal fluids.

It is common practice to reinject fluid into reservoirs during geothermal energy production, but this practice requires careful monitoring to avoid inducing seismic activity. Emerging technologies, including Enhanced Geothermal Systems (EGS) and Advanced Geothermal Systems (AGS), offer significant future potential but remain in early stages of development and require substantial further investment and technological advancement.

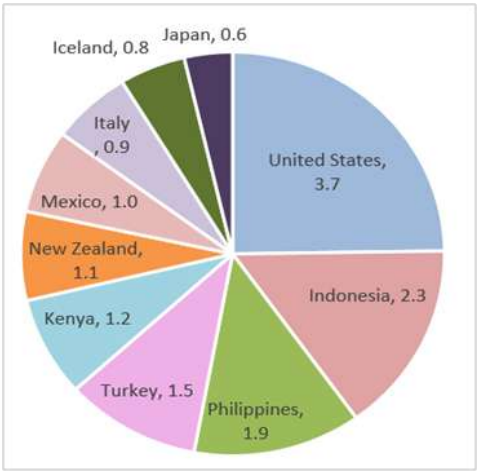


*Fig. 2: Production capacity in GW [data from 8]*

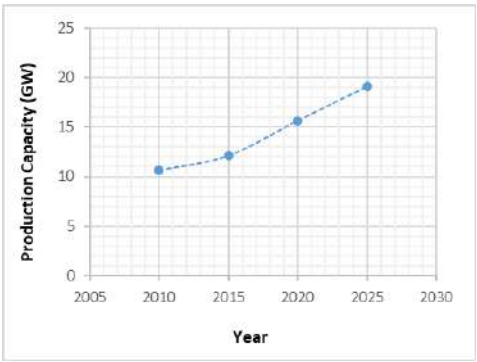


*Fig. 3: World geothermal energy production capacity since 2010 [data from 22]*

### 4.2 Rift Valley Geothermal Prospects

In most East African Rift countries, the use of geothermal energy is limited. For instance, despite established geothermal power plants in Kenya and Ethiopia, geothermal energy contributes only about 1200 MW, indicating significant underutilization given the region's current total electric power utilization, which is close to 20 GW. The East African Rift System (Fig. 4a), which extends for more than 4,000 km from Beira in the south to the Afar Triangle in the north, has significant geothermal energy potential, with high-enthalpy geothermal zones associated with Quaternary volcanoes and rift-related fault zones [8].

The region holds an estimated geothermal potential of 20 GW. However, its expansion has been limited by high investment costs, technical challenges, and policy gaps. Geothermal exploration and resource development are expensive and involve significant financial risk. The cost of completing a single well can exceed $10 million. Deep wells are even more costly because the rock becomes harder to drill as depth increases. The risk of failure is high compared to other energy resource developments. Geothermal technologies are still evolving and will take time to reach maturity, at which point they will become competitive both technically and financially with other established energy technologies.

With the maturation of geothermal technology, many geothermal resources, such as those in the East African Rift, are becoming more economically viable to develop, enabling the exploitation of the region's vast geothermal prospects, which exhibit high temperature gradients of 60-110 °C/km [23]. Within the Main Ethiopian Rift alone, more than 120 geothermal prospects have been identified, with an estimated power generation potential of nearly 10 GW [8,24]. The Ethiopian Rift is projected to have the highest geothermal potential (Fig. 4b), as it represents the most advanced stage of rift development compared with the central Main Ethiopian Rift. Approximately 500 hydrothermal manifestations have been documented, and the northernmost segment is expected to host the greatest geothermal potential [8].

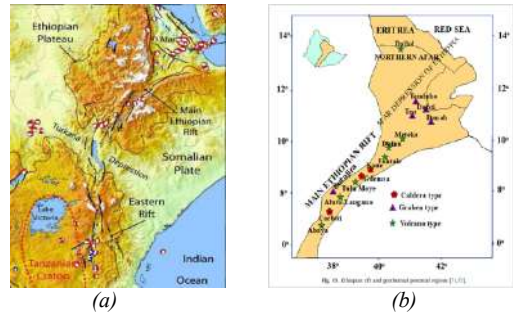


(a) (b)

*Fig. 4: Regional maps: a) East African rift system [25], and b) Ethiopian rift geothermal potential regions [26,27]*

### 4.3 Ethiopian Rift Energy Production

Ethiopia's current geothermal energy generation is still only a few megawatts, far below its vast potential. To date, the Aluto-Langano geothermal field, located about 200 km southeast of Addis Ababa, is the only producing field. Deep exploratory drilling reached depths of up to 2,500 m and encountered temperatures of up to 350°C [28]. Five wells were confirmed as productive, mostly within permeable zones between 2,000 and 2,500 m (Table 1).

The field exhibited a very high geothermal temperature gradient of 99-148 °C/km. A 7.3 MW pilot power plant was commissioned in 1999; however, due to technical and operational challenges, sustained production rarely exceeded about 3 MW [24,29]. Renewed drilling confirmed additional high-temperature resources with power generation potential of over 100 MW [28,30]. Despite this progress, geothermal energy production continues to face challenges related to reservoir management and plant performance [8].

*Table 4.1: Aluto-Langano geothermal wells [8]*

| Parameter | Well Number | | | | | | | |
|---|---|---|---|---|---|---|---|---|
| | LA1 | LA2 | LA3 | LA4 | LA5 | LA6 | LA7 | LA8 |
| Elevation from sea level (m) | 1601 | 1724 | 1921 | 1956 | 2038 | 1962 | 1891 | 1896 |
| Total depth (m) | 1317 | 1602 | 2144 | 2061 | 1867 | 2202.8 | 2448.5 | 2500 |
| Maximum hole temperature (°C) | - | - | 315 | 230 | - | 320 | 228 | 268 |
| Well status | NP | NP | P | P | NP | P | P | P |
| Producing zone (m) | - | - | 2000–2122 | 1445–1800 | - | 2000–2200 | 2100–2300 | 2300–2500 |
| Average thermal gradient (°C/Km) | | | 137 | 114 | | 134 | 88 | 97 |
| Productive = P, Non-productive = NP | | | | | | | | |

The temperature profiles of six wells in the Aluto–Langano geothermal field, shown in Fig. 5, were obtained after long-term discharge testing and therefore represent stabilized formation temperatures. The profiles show pronounced nonlinearity, with decreasing temperature gradients with depth. In some wells, notably LA-7 and LA-5, deeper sections even exhibit negative temperature gradients, indicating localized cooling with increasing depth. Such anomalous thermal behavior deviates from a purely conductive geothermal gradient and reflects strong lateral variations in subsurface temperature distribution within the reservoir. These variations are primarily controlled by the spatial arrangement of heat sources, fluid circulation pathways, and structural heterogeneity.

The W–E cross-sectional temperature contour map in Fig. 6 further illustrates this behavior by delineating a high-temperature core concentrated in the central part of the geothermal field, surrounded by comparatively cooler peripheral zones. Consequently, wells drilled closer to the central region (LA-3 and LA-6) intersect higher-temperature formations, whereas those toward the margins encounter lower reservoir temperatures. This lateral thermal zonation explains the observed nonlinear and locally inverted temperature gradients in the well profiles.

Overall, the combined well-temperature data and the cross-sectional thermal-contour map highlight the importance of lateral heat transfer and reservoir-scale convection in controlling the thermal structure of the Aluto–Langano geothermal system. Similar volcanic complexes along the rift valley are common and can host geothermal systems [23]. Currently, expansion work at the Aluto–Langano field is continuing, and drilling of new wells is expected to reach 70 MW production in two phases [28].

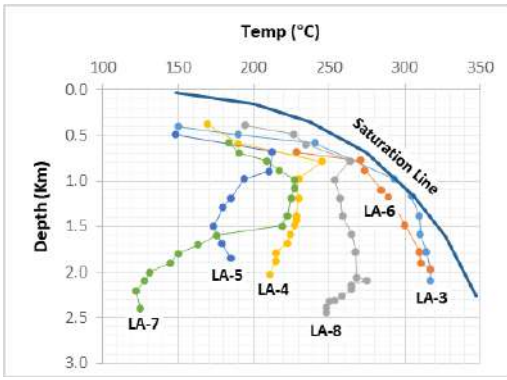


*Fig. 5: Thermal profiles of wells at Aluto-Langano field, redrawn from Teklemariam et al. [29]*

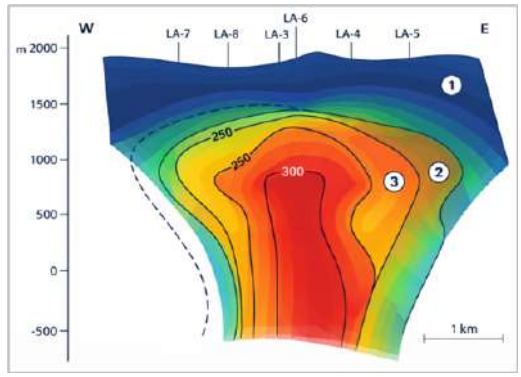


*Fig. 6: W–E cross-sectional temperature contour map of Aluto–Langano geothermal field, redrawn from Teklemariam et al. [29]*

The second-most-explored geothermal field in Ethiopia is Tendaho in the Afar region. Exploratory drilling identified reservoir temperatures exceeding 250°C [31]. Shallow productive wells were sufficient to support a proposed 5 MW pilot plant, while the deeper reservoir was estimated to have a potential of around 20 MW [32,33]. Nevertheless, full commercial development at Tendaho has not yet occurred, largely due to infrastructure and financial constraints. Another new geothermal project is Tulu Moye, located in the central part of the Main Ethiopian Rift. Exploratory drilling has confirmed reservoir temperatures approaching 200°C. Development is planned in phases, beginning with a 50 MW demonstration plant based on 12 production wells. Later phases aim to expand capacity to 150 MW, with long-term projections reaching up to 520 MW [34]. Additional high-potential prospects include Corbetti, Abaya, Fantale, and Dofan. These areas exhibit strong surface manifestations, such as fumaroles, hot springs, and altered ground, along with geophysical evidence of high-temperature reservoirs. However, all remain at pre-commercial stages [8].

Most geothermal power plants worldwide rely on conventional geothermal systems with a technology readiness level (TRL) of 8 or higher. In these systems, fluid circulation through reservoir rocks depends solely on natural permeability. Insufficient or highly heterogeneous permeability, therefore, poses a major upfront financial risk, primarily due to the high cost and uncertainty of success in exploratory and production drilling. To address this challenge, the geothermal industry has developed advanced technologies that enhance or artificially create reservoir permeability, enabling effective fluid circulation and expanding the range of economically viable geothermal resources. Furthermore, as the development of geothermal resources in countries like Ethiopia becomes profitable, these upfront risks must be mitigated through the involvement of Independent Power Producers (IPPs). The IPPs bring expertise, risk-sharing mechanisms, and private capital to the geothermal industry, transferring drilling and resource risks from the public sector to private companies.

### 4.4 New Technologies

Emerging geothermal technologies (Fig. 7), particularly Enhanced Geothermal Systems (EGS) and Advanced Geothermal Systems (AGS), are expected to play a critical role in enhancing both the technical feasibility and economic attractiveness of future geothermal projects.

### 4.4.1 Enhanced Geothermal Systems

Unlike conventional hydrothermal geothermal systems, EGS (TRL 7) is designed for regions where naturally occurring formation fluids are absent. It enables heat extraction from high-temperature rock formations with very low natural permeability and porosity, commonly referred to as hot dry rock [34]. An EGS facility comprises two main integrated components: an engineered subsurface heat-exchange system created through reservoir stimulation and a surface system that converts the recovered heat into electricity [8].

Conventional geothermal resources, by contrast, rely on the natural coexistence of three fundamental elements: a sufficient heat source, a permeable fracture network within the rock, and mobile subsurface fluids. In such systems, natural fractures and circulating fluids are the primary means of transporting heat from depth to the surface. However, the presence and long-term sustainability of these three components depend on complex geological conditions and are further influenced by operational practices during the production phase. These natural and operational constraints significantly limit the geographic distribution and broad-scale utilization of conventional geothermal resources.

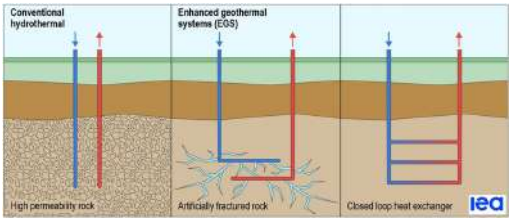


*Fig. 7: Conventional hydrothermal and new geothermal systems [21]*

A major advantage of EGS is its lower development risk compared with traditional geothermal projects. Because the reservoir is created artificially, developers can select suitable geological formations and engineer the heat-exchange system based primarily on temperature gradients and rock properties, rather than depending entirely on the presence of naturally developed hydrothermal reservoirs. This greater level of control allows for more predictable project outcomes and makes EGS particularly attractive to investors [35]. Consequently, EGS and related advanced geothermal technologies represent a transformative pathway for expanding geothermal deployment well beyond the limits of conventional hydrothermal settings.

### 4.4.2 Advanced Geothermal Systems

The AGS (TRL 6) extracts heat primarily by thermal conduction through the well casing, thereby eliminating the material exchange between the circulating fluid and the surrounding reservoir rock. By avoiding direct fluid–rock interaction, AGS significantly reduces many of the complexity and environmental challenges associated with conventional systems and EGS, offering a more environmentally friendly approach to geothermal heat recovery. These systems operate within fully sealed subsurface loops, allowing developers to deploy AGS in a manner similar to EGS by selecting appropriate geological formations and designing the heat-exchange configuration accordingly [36]. An AGS typically utilizes one or more wells drilled into hot rock, within which a working fluid circulates through a closed-loop to transport heat to the surface for both direct-use heating and electricity generation.

The AGS offers several notable advantages that make it particularly attractive for future geothermal development [36]. Because the system is entirely engineered and hydraulically isolated from the surrounding formation, its thermal output can be predicted with relatively high confidence. Unlike stimulation-based geothermal approaches, AGS does not require reservoir stimulation, thereby significantly reducing the risk of induced seismicity and minimizing overall water consumption. In principle, AGS can be deployed in almost any

geological environment where adequate subsurface temperatures exist, which gives it exceptional flexibility and broad geographic applicability. Furthermore, as a fully engineered system, AGS provides substantial opportunities for optimization, scalability, and performance enhancement as technologies continue to improve. Importantly, the system circulates clean working fluids that do not require specialized treatment to control corrosion, limit material degradation and scaling, prevent equipment failure at the surface, and ensure proper wastewater disposal.

Despite these advantages, AGS faces significant technical challenges. These include the potential complexity of downhole well completions and the need to create enough heat-transfer surface area between the closed-loop system and the surrounding hot rock to achieve economically viable heat-extraction rates. Overcoming these challenges will be essential for the successful large-scale deployment of AGS technology.

### 4.4.3 SuperHot Rock (SHR) Engineered Geothermal Systems

Superhot Rock Engineered Geothermal Systems (SHR-EGS or SHR-AGS) are among the most promising methods for scaling clean, economical geothermal energy production [37]. The term "superhot rock" generally refers to systems with formation temperatures above 375°C [38]. SHR (TRL 5) may produce supercritical $H_2O$; however, this would also require pressures above 22 MPa (Fig. 8). Achieving economical EGS or AGS anywhere may not be economically feasible unless power production per well is significantly improved. There are three ways to increase power output per well: increase flow rate, increase flow temperature, or both. Therefore, drilling into SHR resources and extracting high enthalpy fluids (>2100 kJ/kg) could be a potential pathway to cost-competitive geothermal energy worldwide [39]. Superhot rock can generate super-high enthalpy fluids, with specific enthalpy exceeding 2100 kJ/kg [40].

SHR resources are found worldwide, at depths depending on local temperature gradients. The objectives of SHR-EGS or SHR-AGS development projects include achieving high energy generation (>20 MW per well) using high enthalpy fluids, maintaining field operations for over 20 years at an affordable cost of electricity, and reducing the risk of induced seismicity [38]. Nonetheless, significant scientific and developmental uncertainties remain regarding these potentially high-value resources.

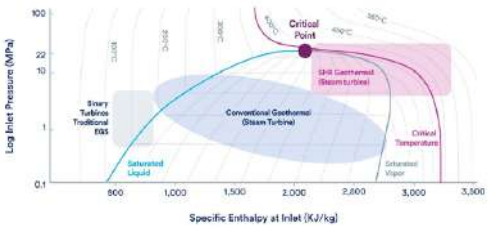


*Fig. 8: Operating envelopes of different geothermal energy production systems [38]*

Despite their enormous promise, substantial scientific, technical, and development uncertainties continue to surround these high-value resources. Major challenges remain in drilling technology, materials performance under extreme temperature and pressure, reservoir sustainability, and long-term system reliability. As a result, while SHR-based geothermal systems represent a transformative opportunity for the future of geothermal energy, their large-scale commercial deployment will depend on continued research, field demonstration, and sustained investment.
Careful site selection is a fundamental requirement for the successful development of SHR resources. Initial testing of SHR technologies and pilot-scale projects should be conducted in well-known geothermal fields and mature developments where extensive geological, geophysical, and geothermal datasets already exist [38]. An equally important factor is the local depth required to reach SHR conditions, as SHR resources may occur at shallower depths in certain regions (Fig. 9) and thus be more readily

accessible using conventional drilling techniques. The identification and characterization of viable SHR prospects rely on integrated geologic mapping, data from exploratory and offset wells, historical seismic records, and both active and passive seismic surveys.

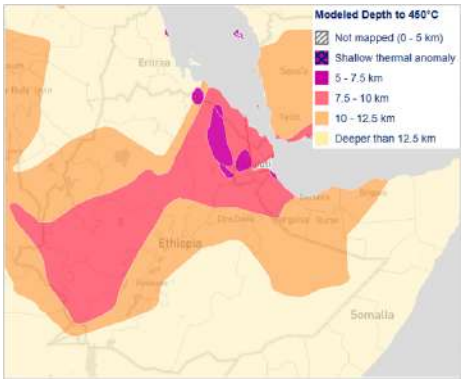


*Fig. 9: Ethiopian map of areas with 450°C super-hot rocks [43]*

Although drilling into SHR formations has been demonstrated by pushing the limits of current drilling technologies, numerous technical challenges remain for the effective and reliable development of these resources. Recent SHR drilling projects have commonly encountered short drill-bit life caused by extreme temperatures, as well as reduced rates of penetration resulting from accelerated bit wear and performance degradation [41]. In addition, casing failures are frequently observed in SHR wells, often driven by severe thermal cycling and cold-water quenching [8,42]. Another major limitation of existing technology is the difficulty of achieving accurate directional drilling for the creation of engineered SHR reservoirs, which is essential for establishing effective heat-exchange systems by maximizing a well's lateral reach to intersect more vertical fractures. Addressing these challenges is critical for enabling the large-scale commercial deployment of SHR-based geothermal energy systems.

## 5. Conclusions

This study shows that long-term energy security and climate resilience in Ethiopia cannot be achieved solely through continued reliance on hydropower. While hydropower has enabled major gains in clean electricity generation and rural electrification, its high sensitivity to climate variability and prolonged drought exposes the national power system to growing reliability risks. Natural gas and geothermal energy are strategic, complementary resources that can stabilize electricity supply, support industrial development, and strengthen economic resilience. Ethiopia's natural gas reserves, coupled with advancing gas-to-power, refinery, and fertilizer infrastructure, offer a timely opportunity to establish a reliable transitional energy source that can respond rapidly to fluctuations in power demand. At the same time, the country's vast geothermal potential within the East African Rift offers a scalable, low-carbon baseload option with long-term sustainability benefits. Emerging technologies such as EGS and AGS systems further expand the future role of geothermal energy beyond conventional hydrothermal limitations. Achieving a balanced and resilient energy portfolio will require coordinated investment, regulatory reform, and sustained technological development.

## 6. Implementation Roadmap and Recommendations

A phased implementation strategy is essential to diversify Ethiopia's energy mix while maintaining grid stability and economic feasibility. In the short term (2025–2030), continued development of domestic natural gas resources can provide dispatchable power to support grid balancing and meet peak demand, thereby facilitating the integration of variable renewable energy sources. In parallel, priority should be given to rapidly deployable technologies, particularly solar and wind power. Expanding large-scale solar plants, rooftop solar systems, and mini-grids can improve electricity access for rural populations

with limited access to electricity (Fig. 1), while targeted wind projects in high-potential corridors can supplement existing generation capacity.

In the medium term (2030–2040), emphasis should shift to large-scale exploration and development of geothermal resources in the Ethiopian Rift Valley. This phase should prioritize comprehensive geothermal exploration, including additional geological mapping and geophysical data collection across the Rift Valley, to support the development of EGS and AGS. Upon completion of the exploration phase, EGS- and AGS-based power generation facilities should be developed. This phase should also focus on establishing risk-mitigation mechanisms and forming partnerships between government entities and IPPs to reduce investment barriers and accelerate project deployment.

In the long term (beyond 2040), efforts should focus on supporting the exploration and development of superhot geothermal resources in the North Afar region, where these resources are highly likely to be accessible without extreme deep drilling (Fig. 9). These efforts should be followed by optimizing a fully diversified and resilient energy system through the integration of advanced energy storage and smart-grid solutions. Collectively, this phased roadmap enhances climate resilience, strengthens energy security, and underpins Ethiopia's long-term sustainable economic growth.

The successful implementation of the roadmap requires a highly skilled, specialized workforce, underscoring a critical human capital gap in Ethiopia's energy sector. To address this challenge, it is recommended that structured partnerships be established among academia, industry, and government to support workforce development. Universities and research institutions can provide targeted education and applied research, while industry partners contribute hands-on training, technology transfer, and operational expertise. Government agencies can facilitate this collaboration through supportive policies, dedicated funding mechanisms, and long-term workforce planning. Such an integrated approach would strengthen local technical capacity, reduce reliance on foreign expertise, enhance project sustainability, and support the effective deployment of advanced technologies for non-hydropower energy resource development.

**Nomenclature**

Acronyms

**AGS** Advanced Geothermal Systems
**BOG** Boil-Off Gas
**EGS** Enhanced Geothermal Systems
**IPP** Independent Power Producer
**LNG** Liquefied Natural Gas
**SHR** SuperHot Rock
**TRL** Technology Readiness Level

**Acknowledgements**

The author gratefully acknowledges the University of Oklahoma for providing institutional support that enabled the successful completion of this study.

**Declaration of Generative AI Technologies**

During the preparation of this article, the author used AI tools to improve the readability, language and graphics of the manuscript. After using the tools, the author reviewed and edited the content as needed and take full responsibility for the content of the published article.

**REFERENCES**

1. World Bank. (2019). Ethiopia energy sector review. World Bank Group.
2. Ethiopian Electric Power (EEP). (2023). Annual power system statistics report. Ethiopian Electric Power.
3. International Energy Agency (IEA). (2022). Africa Energy Outlook 2022. IEA.
4. Addis Ababa City Administration. (2021). Reppie waste-to-energy project technical report. Addis Ababa.
5. African Development Bank (AfDB). (2020). Ethiopia renewable energy development status. African Development Bank.

6. Conway, D., Dalin, C., Landman, W. A., & Osborn, T. J. (2017). Climate and hydropower variability in East Africa. Climatic Change, 142(3–4), 643–658.
7. Gebreegziabher, Z., Mekonnen, A., Deribe, R., & Abera, S. (2018). Impact of drought on hydropower generation in Ethiopia. Energy Policy, 121, 236–244.
8. Benti, N. E., Woldegiyorgis, T. A., Geffe, C. A., Gurmessa, G. S., Chaka, M. D., & Mekonnen, Y. S. (2023). Overview of geothermal resources utilization in Ethiopia: Potentials, opportunities, and challenges. Scientific African, 19, e01562.
9. International Renewable Energy Agency. (2020). Geothermal development in Eastern Africa: Recommendations for power and direct use. Abu Dhabi, United Arab Emirates.
10. Anyango, A. (2025, January 22). Ethiopia identifies natural gas in Ogaden region. Pumps Africa.
11. Worldometer. (n.d.). Ethiopia natural gas reserves, production and consumption statistics. Worldometer.
12. Anyango, A. (2022, August 28). Ethiopia discovers 7 trillion cubic feet of natural gas in Ogaden. Pumps Africa.
13. Tadesse, F. (2025). GCL of China to build $2.5 billion oil refinery in Ethiopia. Bloomberg News.
14. Norways, K. (2025, October 6). Ethiopia to construct first oil refinery with Chinese partner. S&P Global Commodity Insights.
15. Glasson, J., Therivel, R., & Chadwick, A. (2013). Introduction to environmental impact assessment (4th ed.). Routledge.
16. American Society of Mechanical Engineers (ASME). (2018). ASME B31.8: Gas transmission and distribution piping systems. ASME.
17. Mokhatab, S., Mak, J. Y., Valappil, J. V., & Wood, D. A. (2014). Handbook of liquefied natural gas (2nd ed.). Gulf Professional Publishing.
18. International Maritime Organization (IMO). (2016). International code for the construction and equipment of ships carrying liquefied gases in bulk (IGC Code). IMO.
19. Bouabidi, Z., Al-Musleh, E. I., Al Momani, F., Al-Sobhi, S., & Karimi, I. A. (2024). Managing jetty boil-off gas for more sustainable LNG export terminals. ACS Sustainable Chemistry & Engineering, 12(32).
20. Hasan, M. M. F., Zheng, A. M., & Karimi, I. A. (2009). Minimizing boil-off losses in liquefied natural gas transportation. Industrial & Engineering Chemistry Research, 48(21).
21. International Energy Agency. (2024). The future of geothermal energy. Paris.
22. Huttrer, G. W. (2021). Geothermal power generation in the world 2015–2020 update report. In Proceedings of the World Geothermal Congress 2020+1 (pp. 1–17). Reykjavík, Iceland.
23. Elbarbary, S., Abdel Zaher, M., Saibi, H., Fowler, A.-R., & Saibi, K. (2022). Geothermal renewable energy prospects of the African continent using GIS. Geothermal Energy, 10(1), 8.
24. Teklemariam, M., & Kebede, S. (2010). Strategy for geothermal resource exploration and development in Ethiopia. In Proceedings of the World Geothermal Congress (pp. 25–29). Bali, Indonesia.
25. Omenda, P. (2014). Geothermal country update report for Kenya: 2014. UN University Geothermal Training Program, Geothermal Development Co., & Kenya Electricity Generating Co., Kenya.
26. Ministry of Water and Energy. (2012). Scaling-up renewable energy program: Ethiopia investment plan. Addis Ababa, Ethiopia.
27. Ethiopian Electric Power Corporation. (2014). Ethiopian power sector overview. Addis Ababa, Ethiopia.
28. Samrock, F., Grayver, A. V., Cherkose, B., Kuvshinov, A., & Saar, M. O. (2020). Aluto-Langano geothermal field, Ethiopia: Complete image of the underlying magmatic–hydrothermal system revealed by revised interpretation of magnetotelluric data. In Proceedings of the World Geothermal Congress (pp. 12–19). Reykjavík, Iceland: UNU-GTP.

29. Teklemariam, M., Battaglia, S., Gianelli, G., & Ruggieri, G. (1996). Hydrothermal alteration in the Aluto-Langano geothermal field, Ethiopia. Geothermics, 25, 679–702.
30. Biru, M. F. (2016). Analysis of well testing, temperature and pressure in high-temperature wells of Aluto-Langano, Ethiopia. UNU-GTP, Reykjavík, Iceland.
31. Gebregziabher, Z. (1997). Ethiopian geothermal resources and their characteristics. Transactions of the Geothermal Resources Council, 21, 361–363.
32. Ali, S. (2005). Geochemical studies of the Tendaho geothermal field. In Proceedings of the World Geothermal Congress 2005 (pp. 24–29).
33. Amdeberhan, Y. (2005). Exploration results in the Tendaho geothermal field, Ethiopia. In Proceedings of the World Geothermal Congress 2005 (pp. 24–29).
34. Burnside, N., Montcoudiol, N., Becker, K., & Lewi, E. (2021). Geothermal energy resources in Ethiopia: Status review and insights from hydrochemistry of surface and groundwaters. WIREs Water, e1554, 1–27.
35. Olasolo, P., Juárez, M. C., Morales, M. P., D'Amico, S., & Liarte, I. A. (2016). Enhanced geothermal systems (EGS): A review. Renewable and Sustainable Energy Reviews, 56, 133–144.
36. White, M., Vasyliv, Y., Beckers, K., Martinez, M., Balestra, P., Parisi, C., Augustine, C., Bran-Anleu, G., Horne, R., Pauley, L., Bettin, G., Marshall, T., & Bernot, A. (2024). Numerical investigation of closed-loop geothermal systems in deep geothermal reservoirs. Geothermics, 116, 102852.
37. Cladouhos, T. T., & Callahan, O. A. (2024). Heat extraction from superhot rock – Technology development. In Proceedings of the 49th Workshop on Geothermal Reservoir Engineering (SGP-TR-227). Stanford University, Stanford, California.
38. Cladouhos, T. T., & Callahan, O. A. (2023). Heat extraction from superhot rock: A survey of methods, challenges, and pathways forward. GRC Transactions, 47.
39. Cladouhos, T.T., Petty , S., Bonneville, A., Schultz, A., and Sorlie, C.F. "Sup er Hot EGS and the Newberry Deep drilling Project." Proceedings: 43rd Workshop on Geothermal Reservoir Engineering, Stanford University, Stanford, California (2018).
40. Banks, G., and Ball, P.J., (2023). Superhot Rock Energy Glossary. CATF. Online resource, accessed, November 2023.
41. Garcia, J., Hartline, C., Walters, M., Wright, M., Rutqvist, J., Dobson, P. F., & Jeanne, P. (2016). The Northwest Geysers EGS demonstration project, California—Part I: Characterization and reservoir response to injection. Geothermics, 63, 97–119.
42. Ingason, K., & Árnason, A. B. (2022). Casing failures in high temperature wells. GRC Transactions, 46.
43. Clean Air Task Force. (2025). Global map for next-generation geothermal projects. Retrieved November 29, 2025

## Advancing Chemical Engineering for Ethiopia's Sustainable Industrial Future

The Ethiopian Society of Chemical Engineers (ESChE) is the national professional community dedicated to promoting excellence in chemical engineering through research, innovation, professional collaboration, and capacity building.

## Celebrating 25 Years of active Professional Community

For twenty-five years, ESChE has connected engineers, academics, students, and industry leaders working together to strengthen Ethiopia's industrial and technological development.

**Anniversary Theme:**
**Chemical Engineering for Circular Economy Transition in Ethiopia**

Ethiopian Society of Chemical Engineers, College of Technology and Built Environment,
Addis Ababa, Ethiopia